의학박사 학위논문

# The role of arginine vasopressin receptor 1B (AVPR1B) unveiled by the transcriptome analysis in tumorigenesis of silent corticotroph adenomas

# 무증상 ACTH 분비 선종에서 전사체분석을 통해 밝혀진 AVPR1B 의 역할 규명

2020년 2월

서울대학교 융합과학기술대학원

분자의학 및 바이오제약학과

김 정 희

# The role of arginine vasopressin receptor 1B (AVPR1B) unveiled by the transcriptome analysis in tumorigenesis of silent corticotroph adenomas

지도교수 박 경 수

이 논문을 의학박사 학위논문으로 제출함

2020년 2월

서울대학교 융합과학기술대학원

분자의학 및 바이오제약학과

김정희

김 정 희 의 의학박사 학위논문을 인준함

2020년 2월

위 원 장 신찬수 (인)

부 위 원 장 박경수 (인)

위 원 김태유 (인)

위 원 김상완 (인)

위 원 백자현 (인)

# ABSTRACT

Jung Hee Kim

Department of Molecular Medicine and Biopharmaceutical Sciences

Graduate School of Convergence Science and Technology

Seoul National University

**Background**

Silent corticotroph adenomas (SCAs) represent clinically non-functioning pituitary adenomas (NFPAs) but show ACTH-immunopositive staining without biochemical and clinical manifestation of hypercortisolism. SCAs usually present with mass-related symptoms and display an aggressive course. I aimed to examine the prognosis of SCAs, the distinct gene expression profiling of SCAs compared with null cell adenomas (NCAs), and the role of arginine vasopressin receptor 1B (AVPR1B) through transcriptome analysis.

**Methods**

This clinical study included 433 subjects with clinical NFPAs who underwent primary transsphenoidal surgery. Clinical, biochemical, radiologic, and immunohistochemistry findings were investigated through medical records and compared in subjects with SCAs and those non-SCAs. The risk of recurrence or progression after primary surgery were analyzed using Cox

proportional hazard regression models.

Transcriptome analysis was conducted in fresh-frozen 8 SCA and 15 NCA pituitary tumor tissues using RNA sequencing through the Illumina platform. Differentially expressed genes between SCAs and NCAs were further analyzed via gene ontology enrichment analysis, pathway analysis, and network analysis.

Mouse pituitary corticotroph AtT20 cells were knocked down with AVPR1B siRNA transfection. Subsequently, proliferation, migration, and invasion assays were performed. The effect of AVP and AVPR1B-specific antagonist, SSR149415 on proliferation, migration, and invasion of AtT20 cells.

**Results**

Among 433 subjects with clinical NFPAs, 69 subjects harbored SCAs according to the immunohistochemistry results. Subjects with SCAs were more likely to be females and had higher levels of morning plasma ACTH and cortisol than those without SCAs. There were no significant differences in subjects with and without SCAs regarding the tumor volume, cavernous sinus invasion, and Ki-67 proliferation index. However, subjects with SCAs had approximately 3.3-fold higher risk of recurrence or progression than those without SCAs.

RNA sequencing analysis revealed that 1695 genes were significantly differentially expressed including, 994 up-regulated and 701 down-regulated genes ($|\text{fold change (FC)}| \geq 2$ and false discovery rate (FDR) $< 0.05$). Among

transcription factors, *TBX19 (T-pit)* was highly expressed in SCAs and *POU1F1 (Pit-1), GATA2, NR5A1 (SF-1),* and *NR0B1 (DAX1)* was less expressed in SCAs than NCAs. The genes *AVPR1B, EGFR,* and *POMC* were upregulated in SCAs, whereas *DRD2*, *SSTR3,* and *PCSK2* were down regulated in SCAs. In further gene ontology and pathway analysis, immune-response-related pathway, cancer-related pathway, MAPK cascade, and $G_{\alpha}(q)$ signaling were activated in SCAs, but peptide hormone processing and extracellular matrix formation were suppressed in SCAs.

In AtT20 cells, the knockdown of *AVPR1B* did not affect cell proliferation but decreased ACTH release, migration, and invasion capacity. AVP enhanced the migration capacity while SSR149415 reduced the invasion capacity in AtT20 cells

**Conclusion**

Among subjects with clinical NFPAs, those with SCAs were at a higher risk of recurrence or progression after primary surgery than those without SCAs. AVPR1B may play a role in the aggressiveness as well as ACTH-immunopositivity of SCAs. AVPR1B could become a novel drug target in subjects with refractory SCAs.

**Keywords**: Silent corticotroph adenomas, clinically nonfunctioning adenomas, null cell adenomas, ACTH, AVPR1B

Student ID: 2012-30797

# CONTENTS

# LIST OF FIGURES

# .LIST OF TABLES

# LIST OF ABBREVIATION

ACTH, Adrenocorticotropic hormone

AKT, Serine/threonine kinase (protein kinase B)

AVP, Arginine vasopressin

AVPR1B, Arginine vasopressin receptor 1B

CI, Confidence interval

CRH, Corticotropin-releasing hormone

DEG, Differentially expressed genes

ERK1/2, Extracellular signal-regulated kinase 1/2

FC, Fold change

FDR, False discovery rate

FPKM, Fragments per kilobase per million sequenced reads

FSH, Follicle-stimulating hormone

GAPDH, Glyceraldehyde 3-phosphate dehydrogenase

GH, Growth hormone

GO, Gene ontology

GSEA, Gene set enrichment analysis

GTR, Gross total resection

HR, Hazard ratios

IHC, Immunohistochemistry

KEGG, Kyoto Encyclopedia of Genes and Genomes

LH, Luteinizing hormone

MAPK, Mitogen-activated protein kinase

MEK, Mitogen-activated protein/extracellular signal-regulated kinase kinase

MR, Magnetic resonance

NC, Negative control

NCA, Null-cell adenomas

NFPA, Non-functioning pituitary adenoma

PAGE, Parametric analysis of gene set enrichment

PC/PCSK, Prohormone convertase

POMC, Proopiomelanocortin

qRT-PCR, quantitative real-time polymerase chain reaction

SCA, Silent corticotroph adenomas

SD, Standard deviation

TSH, Thyroid-stimulating hormone

WGCNA, Weighted gene coexpression network analysis

WHO, World Health Organization

# INTRODUCTION

Pituitary adenomas are derived from the anterior lobe of the pituitary gland which consists of pituitary hormone-secreting cells such as growth hormone (GH), prolactin, adrenocorticotropic hormone (ACTH), thyrotropin, and gonadotropins. Pituitary adenomas are common neoplasms accounting for 10-20% of all intracranial tumors (1, 2). The prevalence and incidence of pituitary adenomas is estimated to be about 80-100 cases per 100,000 and 4 case per 100,000 person-years, respectively (1, 3, 4). Pituitary adenomas show the highly variable clinical behaviors. About 50-60% of pituitary adenomas are microadenomas (<10 mm) and remain stable. Pituitary macroadenomas (≥ 1 cm) may grow slowly with or without clinical symptoms. In contrast, a subset of pituitary tumors grow rapidly and aggressive (5). Aggressive pituitary tumors present with multiple recurrences and metastasis, occurring in 0.1%-0.2% of all cases (6).

According to the hormone-secreting cell types, pituitary adenomas are classified into somatotroph, lactotroph, corticotroph, thyrotroph, gonadotroph, null cell, and plurihormonal adenomas (7). From a clinical perspective, pituitary adenomas are classified as functioning adenomas with clinical symptoms of hormone excess such as acromegaly or Cushing's disease or nonfunctioning adenomas with mass-related symptoms such as visual symptoms. Approximately two-thirds of the pituitary adenomas produce clinical relevant excessive hormones (8). Although pituitary adenomas

produce pituitary hormones, the clinical features vary from overt to silent adenomas (9).

Silent pituitary adenomas indicate adenomas that express anterior pituitary hormones or transcription factors-immunopositive staining but do not produce pituitary hormones at a clinically significant level. Silent corticotroph adenomas (SCAs) was the first subtype of silent pituitary adenomas described by Kovacs et al (10). Traditionally, SCAs clinically present with non-functioning pituitary adenomas (NFPAs) but ACTH-immunopositive staining without biochemical and clinical manifestation of hypercortisolism such as Cushing's syndrome. However, the definition of SCAs has changed since 2017. The World Health Organization (WHO) defined SCAs as pituitary adenomas that arise from adenohypophyseal cells of TPIT lineage that express ACTH and other proopiomelanocortin (POMC)-derived peptides (7).

SCAs constitute approximately 3-6% of all pituitary adenomas and 10-20% of clinically NFPAs (11, 12). There are controversies as to whether SCAs are truly silent or not. It has been reported that postoperative adrenal insufficiency occurs in 20%-30% of patients with SCAs (13), suggesting that the local secretion of ACTH from SCAs may suppress normal corticotroph cells (14). However, a recent prospective study found that the hypothalamic-pituitary-adrenal axis function in SCA patients was identical to that in non-SCA patients, suggesting that SCAs were truly nonfunctioning (15).

The reason why tumors synthesize ACTH but do not cause clinical symptoms remain unclear. Several putative mechanisms have been suggested. One theory is that cell originating from SCAs are different from those originating from overt corticotroph adenomas related to Cushing's disease. Overt corticotroph adenomas arise from the corticotroph cells in the anterior pituitary gland, but SCAs may originate from the POMC-producing cells located in the pars intermedia (16). Therefore, the ACTH secretory capacity was low in SCAs. However, this finding that SCAs are derived from an intermediate lobe was not confirmed in subsequent studies (13). Another hypothesis is that SCAs produce high-molecular-weight ACTH, which may interfere with the normal ACTH at the receptor level (17). Other researchers proposed that intracellular degradation of ACTH was increased and exocytosis of hormone from the cell membranes was impaired (10). Currently, the most feasible hypothesis is that there are inefficient POMC cleavage enzymes such as prohormone convertase 1/3 (PC1/3) (18-20). PC1/3 is needed in the post-translational processing of POMC into mature ACTH (21). Previous studies have shown that the gene expression of PC1/3 was down-regulated in SCAs compared with that in overt corticotroph adenomas (18, 20, 22).

SCAs usually present with giant adenomas and marked cavernous sinus invasions and show greater recurrence rates (14, 23, 24). Subjects with SCAs are usually younger and more likely to be females compared to those with

null cell adenomas (NCAs) (25). Previous studies suggested that SCAs were of similar size and invasiveness to NCAs but were associated with greater recurrence rates (12, 13). In another study, SCAs tended to show cavernous sinus invasion and greater progression and/or recurrence than non-SCAs (20, 26). In contrast, other retrospective studies demonstrated no further risk of recurrence in SCAs (27, 28). Moreover, a recent systemic review failed to show a higher recurrence risk of SCAs than those of other NFPAs (29). Thus, it is still controversial whether SCAs are truly aggressive or not.

There have been several attempts to explain the aggressive nature of SCAs. SCAs express a lower level of cyclin-dependent kinase inhibitor 2A (CDKN 2A) and a higher level of cyclin D1 than overt corticotroph adenomas (30). This combination promotes cell proliferation by impairing the G1 phase cell cycle arrest. As a marker of cell growth and survival, galectin-3, a β-galactoside binding protein, is involved in cell adhesion, growth, and apoptosis in pituitary tumors (31). However, SCAs shows lower levels of galectin-3 than overt corticotroph adenomas, which demonstrates the little effect of galectin-3 on SCA behaviors (32). Therefore, there has not yet been a plausible mechanism explaining the aggressiveness of SCAs.

Arginine vasopressin (AVP) as well as corticotropin-releasing hormone (CRH) has been known to be secretagogues for ACTH release (20). Arginine vasopressin receptor 1B (AVPR1B) among three subtypes of AVP receptors (V1a, V1b, and V2) is predominantly expressed in the anterior pituitary

corticotroph cells and mediates ACTH secretion induced by AVP (21-24). AVPR1B has been reported to be overexpressed in ACTH-secreting pituitary adenomas causing Cushing's disease (25), but there is lack of data regarding the expression of AVPR1B in SCAs.

Taken together, I aimed to investigate the prognosis of SCAs and compare its gene expression profiling with NCAs towards explaining the tumorigenesis of SCAs. Furthermore, I hypothesized that AVPR1B, which is the most commonly up-regulated gene in SCAs as revealed by transcriptome analysis, may have a role in the biological behavior as well as ACTH secretion in an *in vitro* study.

# MATERIALS AND METHODS

## Clinical study

*Subjects and methods*

The study included 433 subjects with clinical NFPAs who underwent primary transsphenoidal surgery due to visual symptoms by a single surgeon at the Seoul National University Hospital from May 2010 to April 2018. Clinical NFPAs were defined as no clinical or biochemical evidence of hormone excess such as acromegaly, prolactinoma, or Cushing's syndrome.

This study was a part of a Seoul National University Pituitary Tumor Study (SNU-PIT: IRB no. 1503-040-654). The requirement for written informed consent was waived in subjects who were enrolled in the clinical study but was obtained from study subjects who were enrolled in the transcriptome study, which was conducted as a part of a prospective study.

Clinical, biochemical, radiologic, and pathological characteristics were investigated through medical records. Pituitary and target organ hormones including GH, insulin-like growth factor 1, luteinizing hormone (LH), follicle-stimulating hormone (FSH), estradiol or total testosterone, prolactin, free thyroxine, thyroid-stimulating hormone (TSH), ACTH, and serum cortisol levels were measured by radioimmunoassay or immunoradiometric assay between 8 am and 9 am to assess hormone status. Magnetic resonance (MR) images of the sella turcica with T1- and T2-weighted spin echo were obtained before and after gadolinium-based contrast medium administration

in all subjects. Tumor volume was assessed by multiplying the tumor area on coronal view and the slice thickness on MR images. The mean tumor volume was determined on the basis of two-measurement. The presence of cavernous sinus invasion was detected as per the Knosp classification based on coronal T1-weighted contrast preoperative MR imaging (33). The degree of tumor removal was gauged according to both postoperative MR imaging findings and the surgeons' intraoperative vision. A gross total resection (GTR) was designated if the tumor was completely removed according to the surgeon's view, and there was no residual tumor on immediate postoperative MR imaging. Tumor recurrence was defined as the viable tumor lesion after GTR. Tumor progression was defined as the final volume of the tumor that exceeded 120% of the postoperative volume after subtotal or partial resection. Gamma-knife surgery was performed in cases of recurrent or residual tumors.

*Immunohistochemistry*

Formalin-fixed paraffin-embedded (10% neutral buffered formalin fixed, routinely processed, and paraffin-embedded) tissue sections (2–3 μm thick) were cut for hematoxylin and eosin staining and immunohistochemistry (IHC). Tissue sections were stained with anti-GH, LH, FSH, Prolactin, TSH, ACTH antibodies, and Ki-67 (DAKO, Glostrop, Denmark). IHC staining was performed using a standard avidin–biotin–peroxidase method or Ventana BenchMark ULTRA (Rosche, CA, USA). We used the positive control and for negative antibody control, we omitted primary antibodies. Tumors were

interpreted as positive for hormone expression if the neoplastic cells showed distinct cytoplasmic staining. Ki-67 labeling index was calculated on virtual slides of Leica Biosystems (Aperio Scan Scope System) using the SpectrumPlus nuclear algorithm n9 image analyzer. A rabbit polyclonal anti-AVPR1B antibody (1:200 dilution; ab104365, Abcam) were used for IHC staining for AVPR1B.

*Statistical analysis*

Data are shown as mean ± standard deviation (SD) for continuous variables or the number of subjects (%) for categorical variables. The $\chi^2$ test or student's *t*-test was used to compare the categorical and continuous variables. The Kaplan–Meier survival curve with the log-rank test was used to compare recurrence or progression-free survival between subjects with SCAs and NCAs. Univariate and multivariable Cox proportional hazard regression models were used to assess the risk of recurrence or progression of pituitary adenomas according to immunostaining status. Hazard ratios (HRs) and corresponding 95% confidence interval (CI) are provided. All statistical analyses were performed using SPSS software (version 22, IBM Corp. USA).

**Transcriptome analysis**

*RNA preparation and RNA sequencing analysis*

Initially, I included 11 SCA and 23 NCA patients who underwent primary

transsphenoidal surgery with available fresh frozen tumor tissues. The tumor tissues were placed in plastic tubes immediately after surgical resection and stored at –80℃ in liquid nitrogen. For total RNA sequencing, the total RNA was isolated using QIAzol lysis reagent (QIAGEN, USA). Total RNA quantity, quality, and purity were determined using a spectrophotometer Nanodrop (Rockland, DE, USA) and a 2100 Bioanalyzer (Agilent Technologies, CA, USA). Among 11 SCAs and 23 NCAs, only 8 SCAs and 15 NCAs were conducted for further RNA sequencing due to low RNA quality, respectively. For library preparation for whole-transcriptome analyses, we used the TruSeq Stranded Total RNA with RiboZero Gold sample Preparation Kit according to manufacturer's instructions (Illumina, Catalog No. 20020599) starting from 1000 ng (RIN>7.0) of total RNA. Accurate quantitation of cDNA libraries was performed using the QuantiFluor TM dsDNA System and a Quantus (Promega). The first strand cDNA followed by second strand cDNA were synthesized from purified fragmented RNAs removal with ribosomal RNA. End repair was performed followed by adenylation of 3′ends. Adapters were ligated and PCR was conducted to selectively enrich DNA fragments with adapters and to amplify the amount of DNA in the library. The quality control of generated libraries was conducted using the 4200 TapeStation with D1000 Screen Tape (Agilent Technologies, CA). The libraries were paired-end sequenced by Macrogen lnc (Seoul, Korea) using NovaSeq 6000 sequencing system (Illumina).

RNA-Seq reads were filtered using Trimmomatic (version 0.36). Filtered reads were aligned to the human genome (hg19) using STAR (version 2.5.3a) (34) and gene expressions were calculated using RSEM (version 1.3.1) (35). The GRCh37/hg19 fasta file from UCSC genome browser and annotation gtf file from UCSC refFlat table were used to make STAR and RSEM genome indexes. Fragments per kilobase per million sequenced reads (FPKM)-normalized gene expression were used for the further analysis. Genes with FPKM>1 in at least one sample were selected.

Analyses of FPKM data were conducted using iDEP 0.90, using the R package limma (36). Genes with a |fold change (FC)| ≥ 2 and false discovery rate (FDR) for $\log_2$-transformed (FPKM+1) <0.05 were considered as differentially expressed.

Gene ontology (GO) enrichment analysis was performed using gene set enrichment analysis (GSEA) (37). GSEA was conducted in the pre-ranked mode using a recent faster algorithm based on the fgsea package. The GO database consists of biological process, cellular component, and molecular function. The Kyoto Encyclopedia of Genes and Genomes (KEGG) pathway based on GSEA was conducted. Parametric analysis of gene set enrichment (PAGE) based on PGSEA package was applied using Wikipathways 2019 (38).

Weighted gene coexpression network analysis (WGCNA) was conducted to identify the most illustrative gene expression of each sample in a module

associated with SCAs. In comparison with traditional differential expression analysis, focusing on coexpression gene patterns allows the precise identification of biologically meaningful modules containing related genes. The gene lists within the blue module were further analyzed for pathway enrichment analysis using KEGG and Reactome pathway (39).

*Quantitative real-time polymerase chain reaction (qRT-PCR)*

Total RNA was prepared using QIAzol lysis reagent (QIAGEN, USA). The cDNA synthesis was carried out using a Superscript IV First-strand Synthesis System (Invitrogen, USA). Real-time PCR was performed on the LC480 (Roche, Switzerland) using SYBR Green I master mix (Roche, Switzerland). Gene expression levels were determined relative to glyceraldehyde 3-phosphate dehydrogenase (GAPDH) levels. Analysis was conducted using the ΔΔCT-method according to manufacturer's instructions (Applied Biosystems). Sequences of mRNA-specific primer employed in qRT-PCR analyses are listed in Supplemental Table 1.

*Cell culture and reagents*

Mouse pituitary corticotroph cells (AtT20, Cat No. CCL-89, ATCC, Manassas, VA, USA, kindly provided by Pf. Lee EJ) were cultured with low-glucose Dulbecco's modified Eagle medium with 100 U/mL penicillin, 100 μg/mL streptomycin, and 10% fetal bovine serum. AtT20 cells were

incubated in a humidified incubator at 37°C with 5% $CO_2$. AVP was purchased from Sigma-Aldrich. SSR-149415, a non-peptide AVPR1B-specific antagonist was purchased from Tocris Bioscience.

*AVPR1B gene silencing*

AVPR1B downregulation was performed using AVPR1B predesigned siRNA (Bioneer, Republic of Korea) and Lipofectamine 3000 (Life technologies). Cells were cultured until reaching 70% confluence according to manufacturer's instructions in a medium without antibiotics for 24 hours prior to transfection. Transfection was maintained using RNAi at a final concentration of 20 nM and 0.75 μL/well Lipofectamine 3000 in Opti-MEM® Reduced Serum Medium. As reference control, cells were transfected in the same manner using Negative Control siRNA (siNC, Bioneer, Republic of Korea). Within 48 hours, sufficient mRNA downregulation of AVPR1B and POMC had been achieved as assessed by qRT-PCR. Information on primers employed in qRT-PCR analyses and target sequences of siRNA are listed in Table 10. Cells treated by this procedure were used in further migration experiments.

*Cell proliferation assay*

The effects of siAVPR1B on the proliferation of AtT20 were determined by MTT assay. AtT20 cells ($2\times10^4$ cells/$cm^2$) were plated on 96-well plates.

After 24 hours, cells were treated with siRNA, AVP, or SSR149415 (AVPR1B-specific antagonist) for 24 hours, and then MTT (Sigma-Aldrich, St. Louis, MO, USA) dissolved in phosphate-buffered saline was added to each well at a final concentration of 0.5 mg/mL. The cells were incubated at 37°C for 2 hours. Formazan (formed in plates during the assay) was dissolved in 100 μL dimethyl sulfoxide (DMSO), and a microplate reader (BioTek Instruments, Winooski, VT, USA) was used to read the optical density of each well at 540 nm.

*Migration and invasion assay*

Boyden chamber assay (CytoSelect™ 24-Well Cell Migration and Invasion Assay, Cell Biolabs) was performed according to the manufacturer's protocol. Briefly, $1\times10^5$ cells, which were transfected with 20 nM siRNA for 24 hours or treated with AVP or SSR149415 in the upper chamber were transferred into each Boyden chamber and incubated with 10 ng/mL epidermal growth factor (EGF) as chemoattractant, added to the lower chamber only. After 48 hours, cells remaining on the upper side of the membrane, which had not migrated through the 8.0 μm pores were removed. Migrated or invasive cells were stained with cell staining solution. For the invasion assay kit, the upper surface of the insert membrane was coated with a uniform layer of dried basement membrane matrix solution. Subsequently, the optical density of the extracted staining was measured at 560 nm; the optical density correlated with

the amount of migrated or invasive cells. Each experiment was carried out three times in triplicates.

*Wound healing assay*

To create a confluent cell monolayer (90 – 95% confluence), AtT20 cells were plated on six-well plates for 24 hours. The scratch was made through the cell monolayer using a 200 μL pipette tip. Then, cell migration was observed for 24 hours after treatment with AVP or SSR149415. The migration capacity of cells was evaluated by comparing the wound area at 16 h relative to the area at 0 h at three different points in each well, using the ImageJ public domain software (NIH, Bethesda, MD). Each experiment was carried out three times.

*Western blot analysis*

Total cell lysates were isolated, separated by sodium dodecyl sulfate polyacrylamide gel electrophoresis (SDS-PAGE), and transferred to PVDF membranes (Millipore, Billerica, MA, USA). The membranes were blocked with 5% skim milk for overnight at 4 ℃, and incubated with primary antibodies (1:1,000) including anti-AVPR1B from Abcam, anti-pAKT, anti-AKT, anti-pERK1/2, anti-ERK1/2, anti-pMEK, anti-MEK, and anti-β-actin from Cell Signaling Technology. After washing with TBS-T buffer, membranes were incubated with secondary antibodies (1:5,000) for 1 hour at room temperature. Blots were washed (three times for 10 min each) and

proteins were visualized using an enhanced chemiluminescence kit (Amersham, Piscataway, NJ).

*Statistical analysis*

The Mann–Whitney U test was used to compare continuous variables. Data are shown as mean ± standard error of the mean (SEM). *P* values ≤ 0.05 were considered as an evidence of statistical significance. All statistical analyses were performed using GraphPad Prism 5.03 (GraphPad Software Inc., La Jolla, CA, USA).

## RESULTS

Among a total of 433 subjects with clinical NFPAs, 69 subjects harbored SCAs according to the immunohistochemistry results. I compared the clinical, biochemical, radiological, and pathological characteristics of study subjects with and without SCAs at baseline (**Table 1**). There was no significant difference in age and body mass index (BMI) between the two groups. However, subjects with SCAs were more likely to be female and had higher levels of morning plasma ACTH and cortisol than those without SCAs. Baseline MR images, tumor volume, or the presence of cavernous sinus invasion was not significantly different between the two groups. The proportion of the Ki-67 proliferation index >3% was also similar between the two groups. No significant difference between the two groups was found in terms of the gross total resection rate, the proportion of gamma-knife surgery, or follow-up duration after surgery.

**Table 1**. Baseline characteristics of study subjects with and without silent corticotroph adenomas

| Variables | SCAs (n=69) | Non-SCAs (n=364) | *P* |
|---|---|---|---|
| Age at diagnosis (years) | 50.6 ± 13.5 | 50.7 ± 13.8 | 0.946 |
| Female, n (%) | 55 (79.7%) | 173 (47.5%) | <0.001 |
| BMI ($kg/m^2$) | 25.8 ± 3.9 | 25.3 ± 3.5 | 0.351 |
| Morning plasma ACTH (pg/mL) | 46.7 ± 33.1 | 35.8 ± 21.1 | 0.006 |
| Morning serum cortisol (μg/dL) | 12.4 ± 9.3 | 9.3 ± 6.5 | 0.002 |
| Tumor volume on MRI ($cm^3$) | 12.1 ± 23.8 | 10.3 ± 9.3 | 0.360 |
| Cavernous sinus invasion, n (%) | 34 (49.3%) | 188 (51.6%) | 0.793 |
| Ki-67 ≥ 3 %, n (%) | 11/49 (22.4%) | 55/234 (23.5%) | 0.874 |
| Gross total resection, n (%) | 49 (83.1%) | 194 (73.5%) | 0.290 |
| Gamma-knife surgery, n (%) | 14 (20.3%) | 93 (25.6%) | 0.447 |
| Follow-up duration (years) | 3.3 ± 2.0 | 3.5 ± 2.4 | 0.483 |

Data are shown as mean ± SD or n (%). SCA, silent corticotroph adenoma; BMI, body mass index; MRI, magnetic resonance imaging; ACTH, Adrenocorticotropic hormone.

**Table 2** shows the risk of recurrence or progression of pituitary adenomas according to the pituitary hormone immunopositive status. When comparing the recurrence or progression risk of each hormone immunopositive adenomas with the corresponding immunonegative ones, only subjects with ACTH-immunopositive pituitary adenomas had a higher risk of recurrence or progression than those with ACTH-immunonegative staining (HR 3.34, 95% CI 1.26-8.85) (**Figure 1**). The immunostaining status for the other pituitary hormones such as FSH, LH, TSH, prolactin, or GH was not associated with the prognosis of clinical NFPAs. In multivariate Cox proportional-hazard models, the HRs (95% CI) adjusted for age, female, BMI (model 1) and additionally adjusted for tumor volume and cavernous sinus invasion (model 2) were 3.17 (1.09-9.23) and 3.94 (1.25-12.41), respectively. Subjects with SCAs had a higher risk of recurrence or progression compared with those with non-SCAs although they did not manifest symptoms of Cushing's syndrome.

**Table 2**. Risk for recurrence or progression of pituitary adenomas according to pituitary hormone immunostaining status (n=433)

(a) Univariate analysis

| Immunostaining | N (%) | HR (95% CI) |
|---|---|---|
| ACTH (+) | 69 (15.9%) | 3.34 (1.26-8.85) |
| FSH (+) | 102 (23.6%) | 0.25 (0.03-1.86) |
| LH (+) | 4 (0.9%) | 3.21 (0.43-24.2) |
| TSH (+) | 29 (6.7%) | 0.05 (0.00-105.5) |
| Prolactin (+) | 99 (22.9%) | 0.51 (0.17-1.55) |
| GH (+) | 17 (3.9%) | 1.70 (0.39-7.38) |
| Null cell | 180 (41.6%) | 0.72 (0.28-1.84) |

(b) Multivariate analysis

| Variables | Model 1 | Model 2 |
|---|---|---|
| ACTH-immunopositivity | 3.17 (1.09-9.23) | 3.94 (1.25-12.41) |
| Age (per year) | 0.96 (0.93-0.99) | 0.95 (0.92-0.99) |
| Female (*vs* male) | 0.66 (0.25-1.72) | 0.69 (0.25-1.86) |
| BMI (per kg/m$^2$) | 1.12 (1.01-1.23) | 1.12 (1.01-1.23) |
| Tumor volume (per cm$^3$) | | 1.01 (0.98-1.04) |
| Cavernous sinus invasion | | 2.16 (0.80-5.86) |

Data are shown as hazard ratio (95% confidence interval). HR, hazard ratio; CI, confidence interval. (a) Using Cox proportional-hazards models, reference group: each hormone – immunostaining negative. (b) Model 1, adjusted for age, female, and BMI. Model 2, additionally adjusted for tumor volume and cavernous sinus invasion.

**Figure 1**. Kaplan-Meier curve of recurrence or progression of clinically NFPAs according to ACTH immunostaining status (SCA, silent corticotroph adenomas)

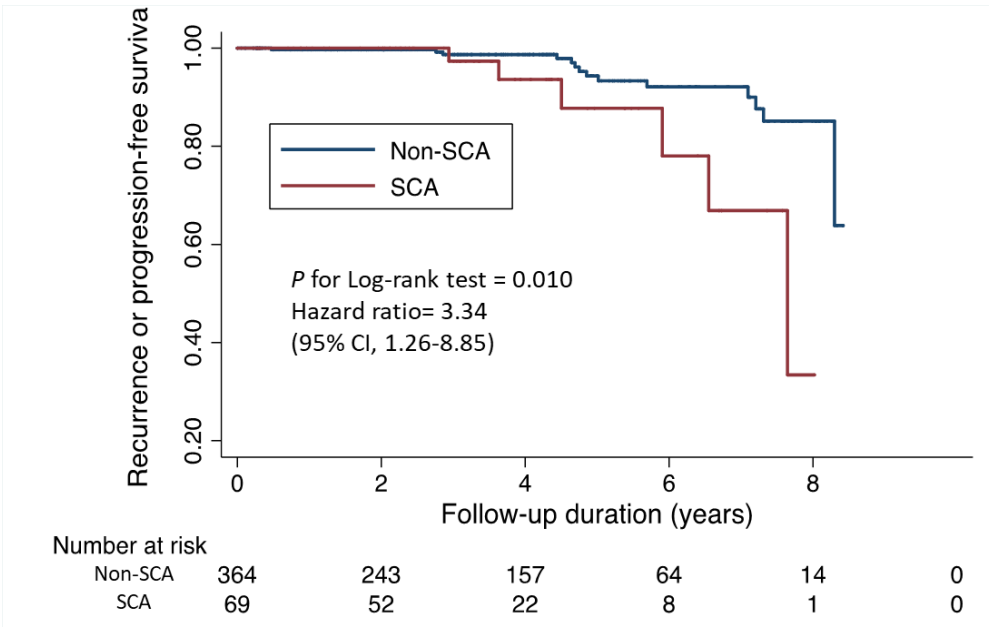

Subsequently, I performed the gene expression profiling using the RNA sequencing analysis to explain the biological behaviors of SCAs. As per the available fresh frozen tumor tissues (SCAs, n=11; NCAs, n=23), only 8 SCAs and 15 NCAs with adequate quality were included in the transcriptome analysis. The baseline characteristics of the study subjects with SCAs and NCAs were not significantly different. However, subjects with SCAs tended to have a greater tumor size and higher proportion of cavernous sinus invasion compared to those with NCAs (**Table 3**).

**Table 3**. Baseline characteristics of study subjects enrolled in the transcriptome analysis (n=23)

| | SCAs (n=8) | NCAs (n=15) | *P* |
|---|---|---|---|
| Age at diagnosis (years) | 56.4 ± 10.0 | 48.8 ± 15.7 | 0.192 |
| Female, n (%) | 8 (100%) | 9 (69.2%) | 0.986 |
| BMI ($kg/m^2$) | 25.4 ± 2.7 | 24.8 ± 4.0 | 0.706 |
| Tumor volume on MRI ($cm^3$) | 16.7 ± 8.0 | 11.5 ± 15.7 | 0.344 |
| Cavernous sinus invasion, n (%) | 8 (100%) | 12 (80%) | 0.957 |
| Morning plasma ACTH (pg/mL) | 51.8 ± 17.7 | 47.8 ± 23.6 | 0.674 |
| Morning serum cortisol (μg/dL) | 14.2 ± 2.5 | 15.1 ± 6.4 | 0.631 |
| Ki-67 (%) | 1.8 ± 1.3 | 2.2 ± 0.9 | 0.540 |

Data are shown as mean ± SD or n (%).SCA, silent corticotroph adenoma; NCA, null cell adenoma; BMI, body mass index.

RNA sequencing analysis identified that 1695 genes were significantly differentially expressed including 994 up-regulated genes and 701 down-regulated genes ($|FC| \geq 2$ and FDR for $\log_2$-transformed (FPKM+1)<0.05). As shown in **Figures 2(a)** and **2(b**), principal component analysis and t-distributed stochastic neighbor embedding plots demonstrated the distinct transcriptome profiling between SCAs and NCAs. Volcano plots showing the magnitude (x-axis) and the statistical significance (y-axis) of the difference in expression of each gene in groups show the different gene expression profiles between the two groups (**Figure 2(c)**. The K-means clustering heatmap based on the 2000 transcripts with the highest variability showed distinct gene expression profiles between the two groups
(**Figure 2(d)).** The 50 most commonly up-regulated and down-regulated genes in SCAs are shown in **Tables 4** and **5**

**Figure 2.** Differentially expressed genes (DEGs) analysis between silent corticotroph adenomas and null cell adenomas. (a) Principal component analysis (b) t-distributed stochastic neighbor embedding plots (c) Volcano plots showing the magnitude (x-axis) and the statistical significance (y-axis) of the difference in expression of each gene in groups (d) Heatmap showing gene expression profiles by K-means clustering based on the 2000 transcripts with the highest variability (A, silent corticotroph adenomas; C, null cell adenomas)

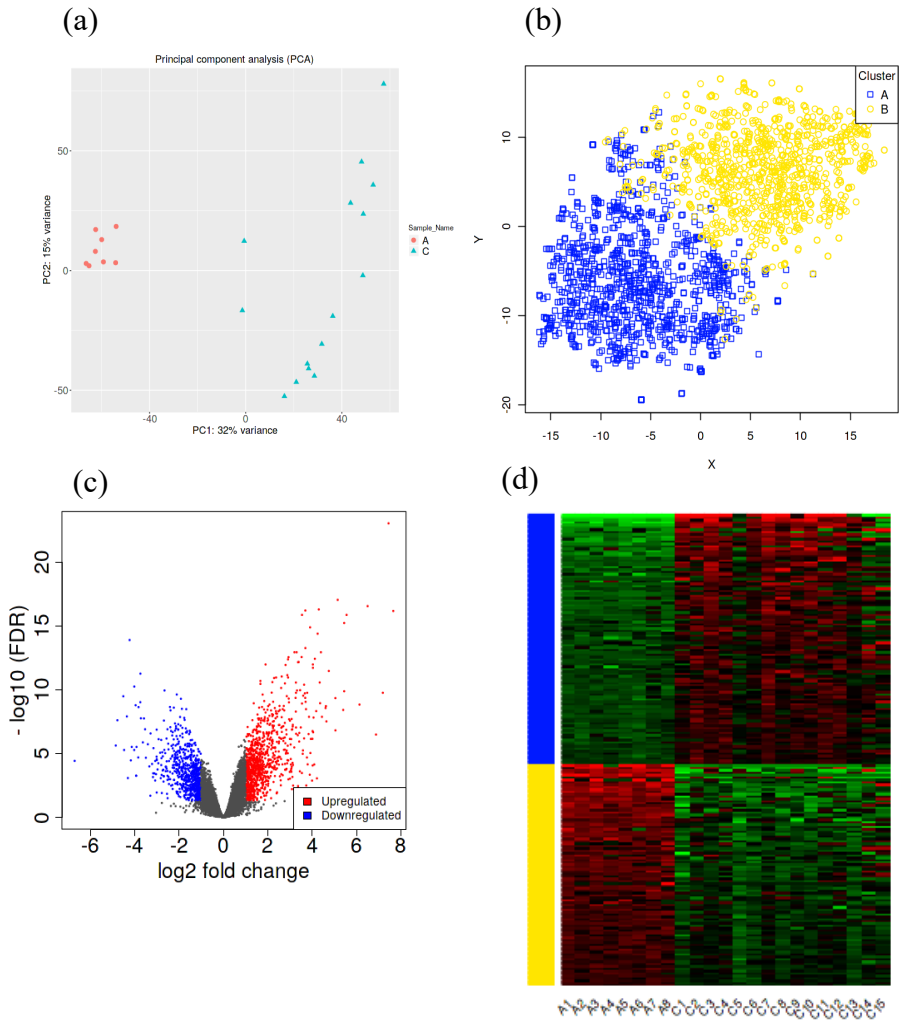

**Table 4**. Up-regulated 50 genes in silent corticotroph adenomas compared with null cell adenomas

| Gene | Gene description | $log_2FC$ | Adjusted *P* |
|---|---|---|---|
| AVPR1B | arginine vasopressin receptor 1B | 7.44 | 9.44E-24 |
| GZMK | granzyme K | 7.66 | 6.87E-17 |
| RASD1 | ras related dexamethasone induced 1 | 7.19 | 1.75E-10 |
| NNAT | neuronatin | 6.88 | 3.27E-07 |
| CALB1 | calbindin 1 | 6.50 | 2.88E-17 |
| NEB | nebulin | 5.55 | 1.40E-16 |
| PCP4L1 | Purkinje cell protein 4 like 1 | 5.44 | 1.33E-10 |
| TBX19 | T-box 19 | 5.44 | 6.03E-16 |
| COL11A1 | collagen type XI alpha 1 chain | 5.40 | 3.88E-09 |
| NWD1 | NACHT and WD repeat domain containing 1 | 5.15 | 9.29E-18 |
| SST | somatostatin | 5.05 | 1.54E-07 |
| SERTM1 | serine rich and transmembrane domain containing 1 | 5.05 | 4.59E-10 |
| ALPK2 | alpha kinase 2 | 4.75 | 3.44E-12 |
| CNKSR3 | CNKSR family member 3 | 4.64 | 3.05E-08 |
| RGS4 | regulator of G-protein signaling 4 | 4.62 | 1.94E-09 |
| ANGPTL7 | angiopoietin like 7 | 4.61 | 2.73E-09 |
| FMO5 | flavin containing monooxygenase 5 | 4.44 | 1.34E-08 |
| AGMO | alkylglycerol monooxygenase | 4.40 | 1.17E-13 |
| SUSD4 | sushi domain containing 4 | 4.36 | 1.15E-09 |
| ONECUT1 | one cut homeobox 1 | 4.34 | 2.74E-11 |
| SSTR1 | somatostatin receptor 1 | 4.30 | 5.20E-17 |
| KRTAP20-4 | keratin associated protein 20-4 | 4.25 | 4.14E-15 |
| HIST3H2BB | histone cluster 3 H2B family member b | 4.22 | 8.83E-04 |
| SLC39A8 | solute carrier family 39 member 8 | 4.18 | 4.80E-09 |
| KRTAP20-2 | keratin associated protein 20-2 | 4.12 | 3.81E-13 |
| PCDH9 | protocadherin 9 | 4.10 | 7.20E-05 |

| | | | |
|---|---|---|---|
| RALYL | RALY RNA binding protein-like | 4.06 | 1.53E-08 |
| GRIK2 | glutamate ionotropic receptor kainate type subunit 2 | 4.05 | 2.17E-07 |
| KRTAP20-3 | keratin associated protein 20-3 | 4.04 | 1.95E-12 |
| CLMP | CXADR like membrane protein | 4.03 | 1.07E-12 |
| POMC | proopiomelanocortin | 4.02 | 8.62E-05 |
| METTL7A | methyltransferase like 7A | 4.02 | 1.76E-07 |
| SCGN | secretagogin, EF-hand calcium binding protein | 4.01 | 7.10E-07 |
| HIST3H2A | histone cluster 3 H2A | 4.00 | 1.33E-03 |
| SCN1B | sodium voltage-gated channel beta subunit 1 | 3.94 | 7.22E-07 |
| MRLN | myoregulin | 3.92 | 9.16E-06 |
| PPFIA2 | PTPRF interacting protein alpha 2 | 3.91 | 1.32E-15 |
| FSTL5 | follistatin like 5 | 3.89 | 4.59E-04 |
| RPRM | reprimo, TP53 dependent G2 arrest mediator candidate | 3.84 | 2.98E-07 |
| DGKK | diacylglycerol kinase kappa | 3.80 | 7.06E-05 |
| PON3 | paraoxonase 3 | 3.77 | 2.04E-05 |
| CARTPT | CART prepropeptide | 3.73 | 3.19E-03 |
| EDN3 | endothelin 3 | 3.72 | 3.36E-09 |
| RAB26 | RAB26, member RAS oncogene family | 3.70 | 8.96E-10 |
| NDST4 | N-deacetylase and N-sulfotransferase 4 | 3.70 | 5.54E-14 |
| ABCA12 | ATP binding cassette subfamily A member 12 | 3.69 | 6.29E-17 |
| HIF3A | hypoxia inducible factor 3 alpha subunit | 3.69 | 4.41E-10 |
| ADGRG2 | adhesion G protein-coupled receptor G2 | 3.67 | 1.94E-10 |
| AGT | angiotensinogen | 3.64 | 4.10E-11 |

FC, fold change

**Table 5**. Down-regulated 50 genes in silent corticotroph adenomas compared with null cell adenomas

| Gene | Gene description | $log_2FC$ | Adjusted *P* |
|---|---|---|---|
| FSHB | follicle stimulating hormone beta subunit | -6.70 | 3.78E-05 |
| NSG2 | neuronal vesicle trafficking associated 2 | -4.85 | 2.37E-06 |
| COL22A1 | collagen type XXII alpha 1 chain | -4.78 | 2.48E-08 |
| LY6H | lymphocyte antigen 6 complex, locus H | -4.51 | 3.30E-10 |
| NR5A1 | nuclear receptor subfamily 5 group A member 1 | -4.47 | 5.30E-06 |
| WFDC2 | WAP four-disulfide core domain 2 | -4.35 | 1.25E-08 |
| RBP4 | retinol binding protein 4 | -4.30 | 8.33E-04 |
| UNC5D | unc-5 netrin receptor D | -4.23 | 1.30E-14 |
| IL13RA2 | interleukin 13 receptor subunit alpha 2 | -4.17 | 3.45E-05 |
| CLCNKA | chloride voltage-gated channel Ka | -4.13 | 3.06E-06 |
| AMIGO2 | adhesion molecule with Ig like domain 2 | -4.02 | 5.30E-06 |
| FGFR1 | fibroblast growth factor receptor 1 | -4.01 | 5.69E-11 |
| KCNA3 | potassium voltage-gated channel subfamily A member 3 | -3.96 | 1.66E-09 |
| CHGA | chromogranin A | -3.91 | 3.06E-06 |
| FOLR1 | folate receptor 1 | -3.84 | 2.03E-05 |
| CCDC69 | coiled-coil domain containing 69 | -3.82 | 2.32E-09 |
| SDC4 | syndecan 4 | -3.74 | 9.59E-10 |
| VAT1L | vesicle amine transport 1 like | -3.74 | 5.55E-12 |
| GPC4 | glypican 4 | -3.72 | 1.75E-08 |
| ADCYAP1R1 | ADCYAP receptor type I | -3.63 | 1.34E-06 |
| FHOD3 | formin homology 2 domain containing 3 | -3.58 | 1.79E-08 |
| EPHB6 | EPH receptor B6 | -3.53 | 1.26E-07 |
| UNC13C | unc-13 homolog C | -3.49 | 2.15E-05 |
| CDH8 | cadherin 8 | -3.40 | 1.88E-06 |
| ALCAM | activated leukocyte cell adhesion molecule | -3.34 | 1.02E-04 |

| | | | |
|---|---|---|---|
| CGA | glycoprotein hormones, alpha polypeptide | -3.29 | 2.02E-02 |
| GATA2 | GATA binding protein 2 | -3.28 | 2.68E-07 |
| SLC10A4 | solute carrier family 10 member 4 | -3.21 | 6.58E-05 |
| PLA2G1B | phospholipase A2 group IB | -3.17 | 6.98E-04 |
| GLRA3 | glycine receptor alpha 3 | -3.16 | 3.55E-04 |
| SPOCK1 | SPARC/osteonectin, cwcv and kazal like domains proteoglycan 1 | -3.15 | 3.80E-06 |
| EDIL3 | EGF like repeats and discoidin domains 3 | -3.07 | 1.31E-03 |
| RAMP1 | receptor activity modifying protein 1 | -3.07 | 3.84E-05 |
| IDH1 | isocitrate dehydrogenase | -3.03 | 4.15E-04 |
| SEMA7A | semaphorin 7A | -3.01 | 1.76E-05 |
| GAL3ST3 | galactose-3-O-sulfotransferase 3 | -3.01 | 1.35E-07 |
| LHB | luteinizing hormone beta polypeptide | -3.01 | 1.13E-02 |
| HPCAL4 | hippocalcin like 4 | -3.00 | 3.29E-05 |
| BAIAP3 | BAI1 associated protein 3 | -2.93 | 5.77E-05 |
| TSPAN1 | tetraspanin 1 | -2.92 | 7.57E-07 |
| GATA3 | GATA binding protein 3 | -2.85 | 8.72E-06 |
| VMO1 | vitelline membrane outer layer 1 homolog | -2.82 | 8.54E-04 |
| NDRG1 | N-myc downstream regulated 1 | -2.80 | 8.70E-07 |
| PNMA6F | PNMA family member 6F | -2.80 | 8.04E-05 |
| MPPED2 | metallophosphoesterase domain containing 2 | -2.79 | 2.32E-05 |
| DPP6 | dipeptidyl peptidase like 6 | -2.78 | 4.71E-04 |
| C2orf80 | chromosome 2 open reading frame 80 | -2.77 | 1.24E-02 |
| PCSK2 | proprotein convertase subtilisin/kexin type 2 | -2.74 | 2.12E-04 |
| AKAP12 | A-kinase anchoring protein 12 | -2.73 | 1.65E-05 |

In **Figure 3**, I explored specific DEGs in terms of tumor development, hormone regulation, and hormone synthesis using FPKM expression levels from the transcriptome analysis. Regarding transcription factors, *TBX19 (T-pit)*, which is the main transcription factor for corticotroph adenoma development, was up-regulated in SCAs. *POU1F1 (Pit-1)* for somatotroph, lactotroph, and thyrotroph adenoma development, and *GATA2, NR5A1 (SF-1),* and *NR0B1 (DAX1)* for gonadotroph adenomas were down-regulated in SCAs. For pituitary hormone-receptor interaction, *POMC*, and *SST* were overexpressed whereas *FSHB, LHB,* and *CGA* (free α-subunit) were under-expressed in SCAs. *GHR,* and *SSTR1* were upregulated, but *IGF1R, SSTR3, DRD2,* and *TRHR* were downregulated in SCAs. *ESR1, AR,* and *NR3C1 (GR)* were up-regulated, while *ESR2* was down-regulated in SCAs. *AVPR1B* and *VAV3* were prominently up-regulated and *PTTG2* which is related with aggressive pituitary adenomas was up-regulated in SCAs. As growth factor receptors, *EGFR* was up-regulated whereas *FGFR1* was down-regulated in SCAs. The expression level of prohormone convertase 1/3 (*PCSK 1/3*), which cleaves ACTH from the POMC polypeptide was not different between the two groups but *PCSK2* expression level was downregulated in SCAs.

**Figure 3**. FPKM expression levels of major DEGs related to (a) transcription factors (b) pituitary hormone (c) pituitary hormone receptor (d) target organ hormone receptors (e) tumorigenesis (f) peptide processing (all FDR <0.05)

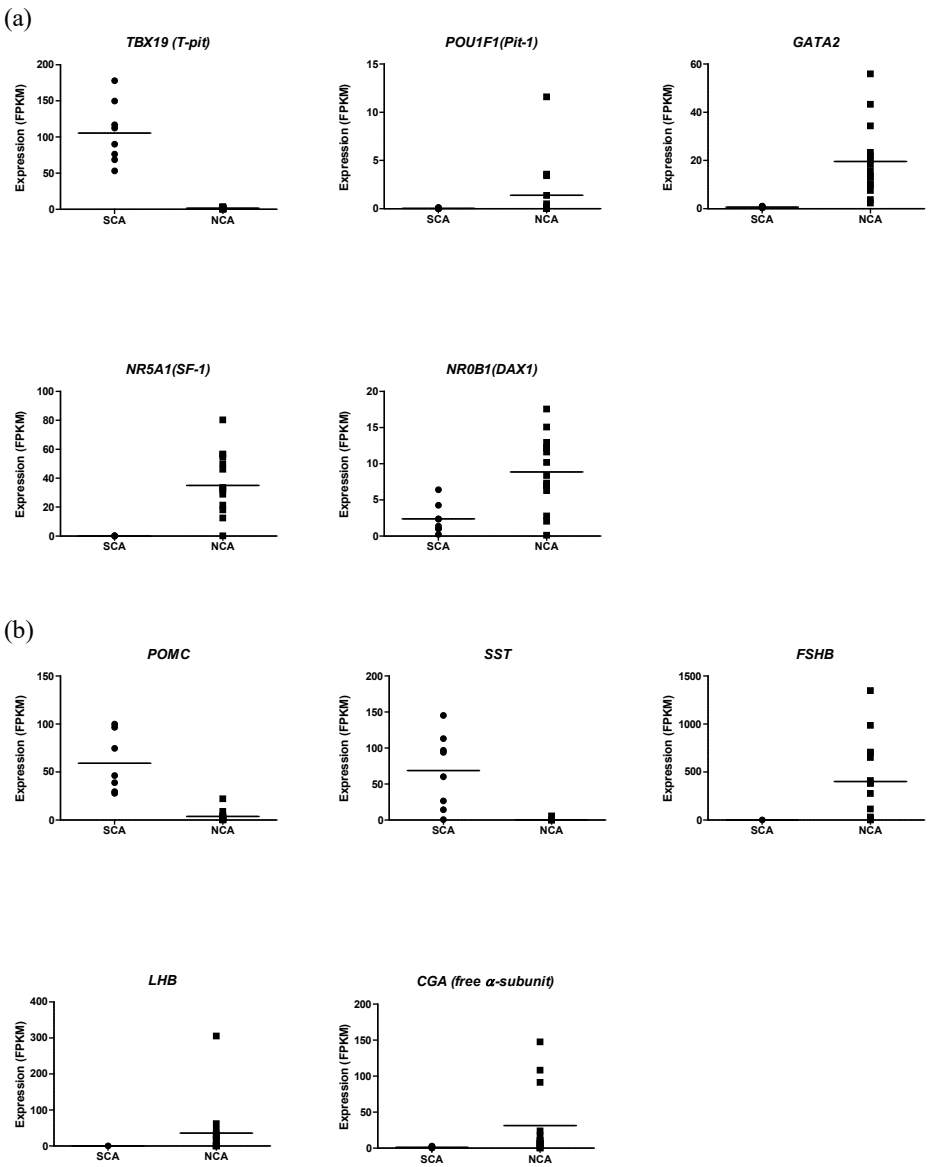

(c)

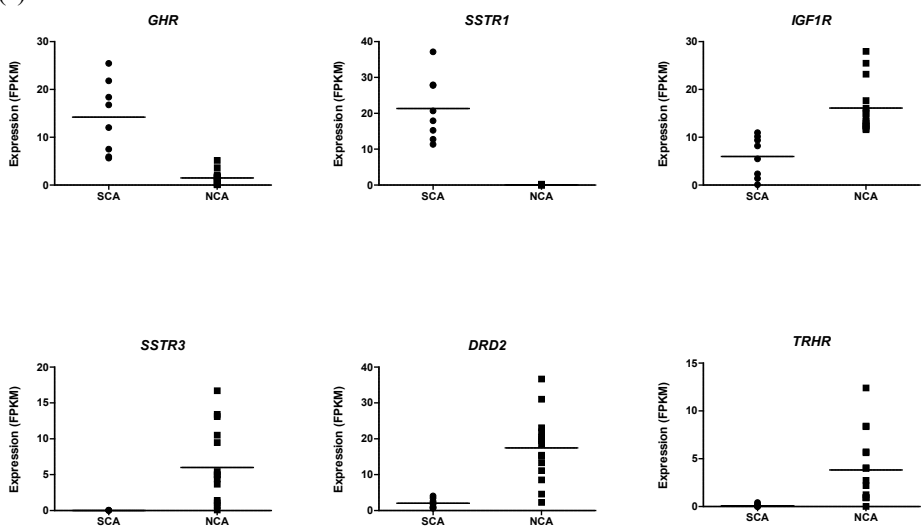
GHR
SSTR1
IGF1R
SSTR3
DRD2
TRHR
Expression (FPKM)
SCA
NCA

(d)

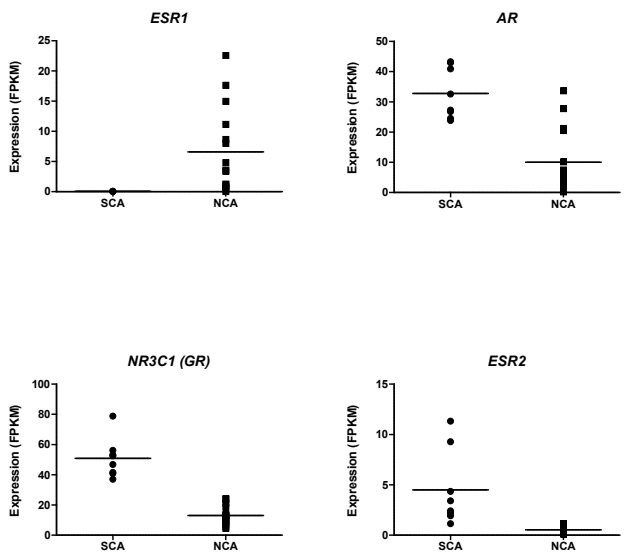
ESR1
AR
NR3C1 (GR)
ESR2
Expression (FPKM)
SCA
NCA

(e)

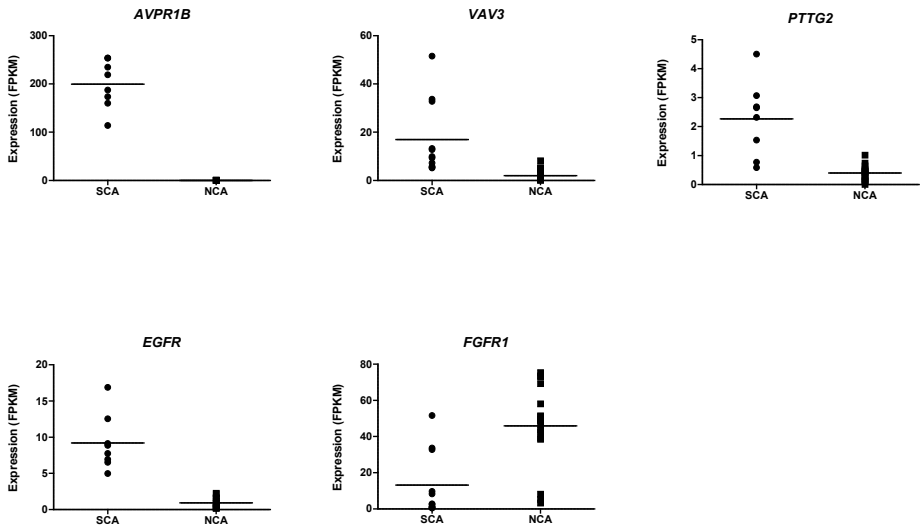


(f)

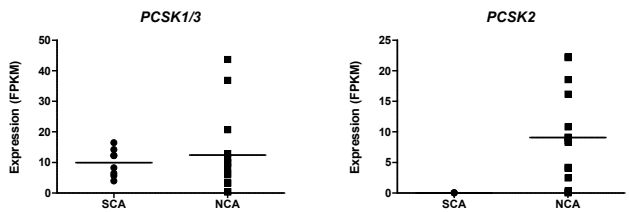


I validated the major up-regulated and down-regulated genes in SCAs by qRT-PCR and were significantly different between the two groups (**Figure 4**).

**Figure 4.** Validation of differentially expressed genes by reverse transcriptase-quantitative polymerase chain reaction: (a) up-regulated DEGs (b) down-regulated DEGs in SCAs (all $P$ <0.05)

(a)

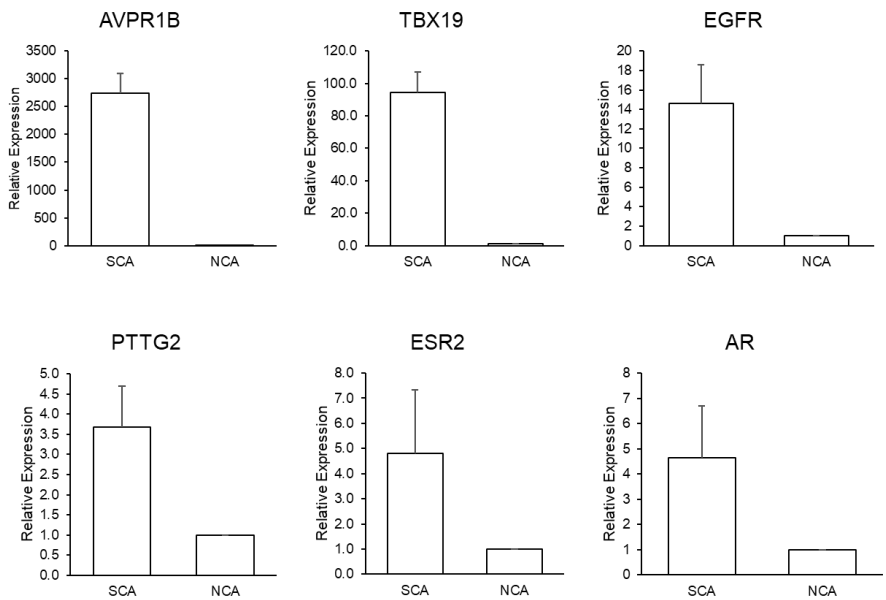


(b)

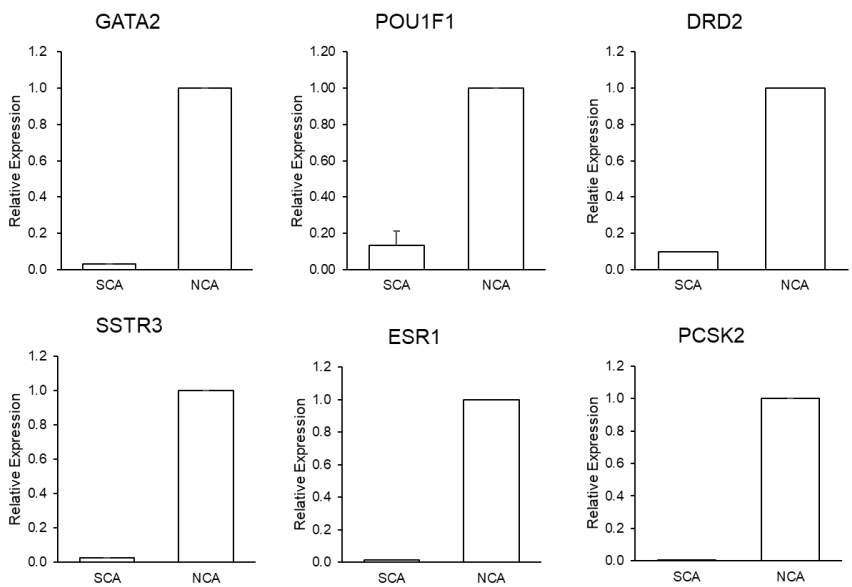

In GO terms of GSEA, peptide hormone processing and extracellular matrix formation were down-regulated in SCAs. However, ion channel activity and immune-related pathway were up-regulated in SCAs (**Table 6**).

The KEGG pathway enrichment analysis of the DEGs using GSEA demonstrated that cell adhesion molecule, extracellular matrix-receptor interaction were down-regulated but insulin signaling pathway, phosphatase D signaling pathway, estrogen signaling pathway, immune-response related pathway and cancer-related pathway were up-regulated in SCAs (**Table 7**).

**Table 6**. Enriched gene ontology (GO) terms of DEGs between silent corticotroph adenomas and null cell adenomas using GSEA (adjusted $P$ <0.05)

| Direction | Pathways | NES | Genes (n) | adjusted $P$ |
|---|---|---|---|---|
| Gene ontology: biological process | | | | |
| Down | Peptide hormone processing | -2.0419 | 25 | 0.036 |
| Down | Female sex differentiation | -2.0044 | 93 | 0.021 |
| Down | Development of primary female sexual characteristics | -1.9378 | 85 | 0.021 |
| Down | Retinoid metabolic process | -1.9002 | 53 | 0.038 |
| Up | Negative regulation of potassium ion transport | 2.0497 | 20 | 0.021 |
| Up | Interleukin-7-mediated signaling pathway | 1.9332 | 26 | 0.033 |
| Up | Positive regulation of neuron death | 1.9106 | 76 | 0.021 |
| Up | Negative regulation of potassium ion transmembrane transport | 1.9082 | 16 | 0.038 |
| Gene ontology: cellular component | | | | |
| Down | Golgi cis cisterna | -2.0087 | 19 | 0.019 |
| Down | Golgi lumen | -1.9214 | 53 | 0.016 |
| Down | Integral component of postsynaptic membrane | -1.8208 | 97 | 0.015 |
| Down | Intrinsic component of postsynaptic membrane | -1.7702 | 102 | 0.016 |
| Up | Nucleosome | 2.1048 | 89 | 0.005 |
| Up | DNA packaging complex | 2.1016 | 96 | 0.005 |
| Up | Sarcoplasmic reticulum | 1.9711 | 60 | 0.001 |
| Up | Sarcoplasmic reticulum membrane | 1.8781 | 33 | 0.019 |
| Gene ontology: molecular function | | | | |
| Down | Collagen binding | -2.1715 | 58 | 0.007 |
| Down | Extracellular matrix structural constituent | -1.9525 | 121 | 0.007 |
| Down | Metallocarboxypeptidase activity | -1.9128 | 17 | 0.049 |
| Up | Ligand-gated cation channel activity | 2.0002 | 72 | 0.007 |
| Up | Cation channel activity | 1.8028 | 228 | 0.007 |
| Up | Potassium channel activity | 1.7851 | 85 | 0.015 |
| Up | Ligand-gated ion channel activity | 1.6838 | 96 | 0.044 |
| Up | Ligand-gated channel activity | 1.6838 | 96 | 0.044 |
| Up | Potassium ion transmembrane transporter activity | 1.6469 | 112 | 0.047 |
| Up | DNA-binding transcription activator activity, RNA polymerase II-specific | 1.6352 | 272 | 0.00 |

**Table 7.** KEGG pathway enrichment analysis of DEGs using GSEA (adjusted $P$ <0.05)

| Direction | Pathways | NES | Genes (n) | adjusted $P$ |
|---|---|---|---|---|
| Down | Cell adhesion molecules | -1.8325 | 89 | 0.0064 |
| Down | Extracellular matrix -receptor interaction | -1.6376 | 67 | 0.042 |
| Up | Type II diabetes mellitus | 2.0359 | 37 | 0.0064 |
| Up | Osteoclast differentiation | 1.8316 | 93 | 0.0064 |
| Up | Systemic lupus erythematosus | 1.83 | 95 | 0.0064 |
| Up | C-type lectin receptor signaling pathway | 1.8106 | 82 | 0.0064 |
| Up | Estrogen signaling pathway | 1.7934 | 100 | 0.0064 |
| Up | T cell receptor signaling pathway | 1.7559 | 76 | 0.016 |
| Up | Alcoholism | 1.7402 | 147 | 0.0064 |
| Up | B cell receptor signaling pathway | 1.7354 | 55 | 0.033 |
| Up | Th17 cell differentiation | 1.7284 | 68 | 0.028 |
| Up | Th1 and Th2 cell differentiation | 1.702 | 55 | 0.039 |
| Up | Chemokine signaling pathway | 1.6996 | 127 | 0.014 |
| Up | Non-small cell lung cancer | 1.6846 | 61 | 0.039 |
| Up | Adipocytokine signaling pathway | 1.6837 | 58 | 0.039 |
| Up | FoxO signaling pathway | 1.6769 | 113 | 0.02 |
| Up | Salmonella infection | 1.6729 | 64 | 0.039 |
| Up | Epithelial cell signaling in Helicobacter pylori infection | 1.6695 | 56 | 0.042 |
| Up | Leishmaniasis | 1.6695 | 47 | 0.042 |
| Up | Pertussis | 1.6671 | 55 | 0.042 |
| Up | Phospholipase D signaling pathway | 1.6615 | 122 | 0.02 |
| Up | Endometrial cancer | 1.6562 | 53 | 0.042 |
| Up | P53 signaling pathway | 1.6504 | 65 | 0.042 |
| Up | Chagas disease (American trypanosomiasis) | 1.6499 | 76 | 0.039 |
| Up | Colorectal cancer | 1.6471 | 75 | 0.039 |
| Up | Toll-like receptor signaling pathway | 1.6265 | 68 | 0.042 |
| Up | Insulin signaling pathway | 1.6259 | 119 | 0.031 |

NES, normalized enrichment score

Using absolute values of FC for GSEA and Wikipathway database, PAGE showed that the IL-6 signaling pathway, AMP-activated protein kinase (AMPK) signaling, non-small cell lung cancer, and mitogen-activated protein kinase (MAPK) cascade was activated in SCAs (**Figure 5).**

**Figure 5.** Parametric analysis of gene set enrichment analysis (PAGE) using Wikipathway enriched pathway analysis of DEGs between SCAs and NCAs (A, SCAs; N, NCAs)

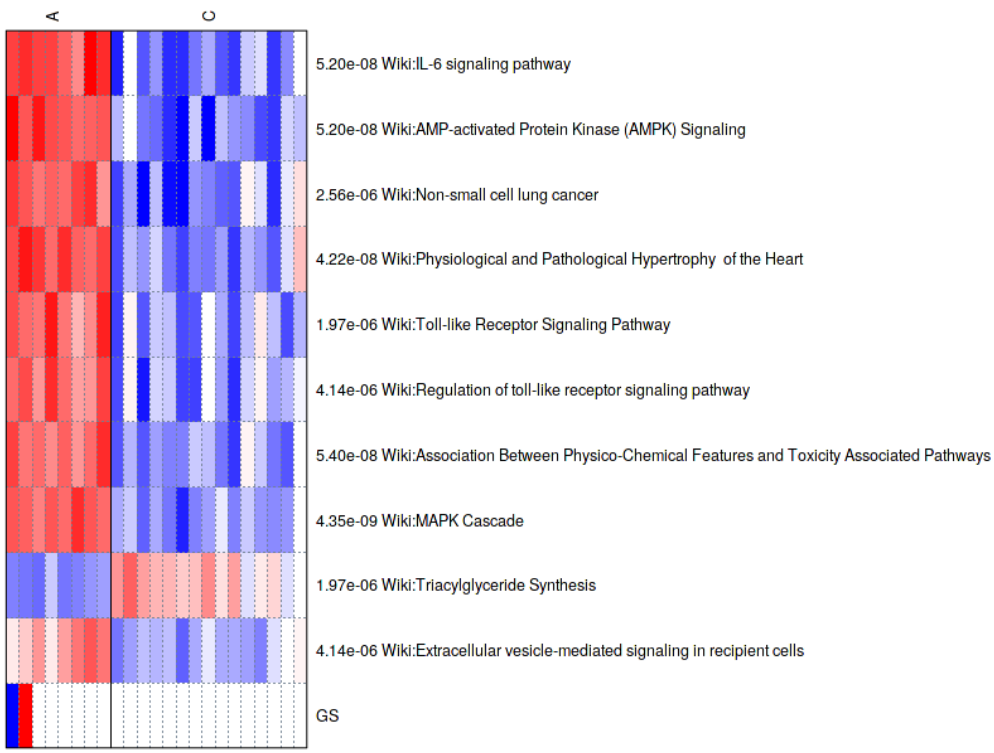

The weighted gene coexpression network analysis (WGCNA) was conducted to identify the most illustrative gene expression of each sample in a module associated with SCAs (**Figure 6**). Using the most variable 958 genes at the soft threshold of 5, four modules with coexpressed genes were identified, and the module with the maximal number of genes is shown in torquoise (n=357). However, in the heatmap of WGCNA, the blue module (n=293) exhibited the most discriminant expression between SCAs and NCAs. Among them, the top highly co-expressed 10 genes were *TBX19, AVPR1B, CTSE, ABCA12, CALB1, TTC39C, SSTR1, GZMK, NEB*, and *NWD1*. Thus, the gene list within the blue module was further analyzed to the pathway enrichment analysis **(Table 8**). The KEGG pathway analysis revealed the neuroactive ligand-receptor interaction, estrogen signaling pathway, and Cushing's syndrome. The Reactome pathway analysis demonstrated the $G_{\alpha}(q)$ signaling events as well as neuronal system-related pathway were up-regulated in SCAs.

**Figure 6.** Weighted gene coexpression network analysis. (a) gene dendrogram and module colors (turquoise, module 1; blue, module 2; brown, module 3; yellow, module 4) (b) heatmap of coexpressed genes according to modules (c) network of top highly co-expressed 10 genes (A, SCAs; C, NCAs)

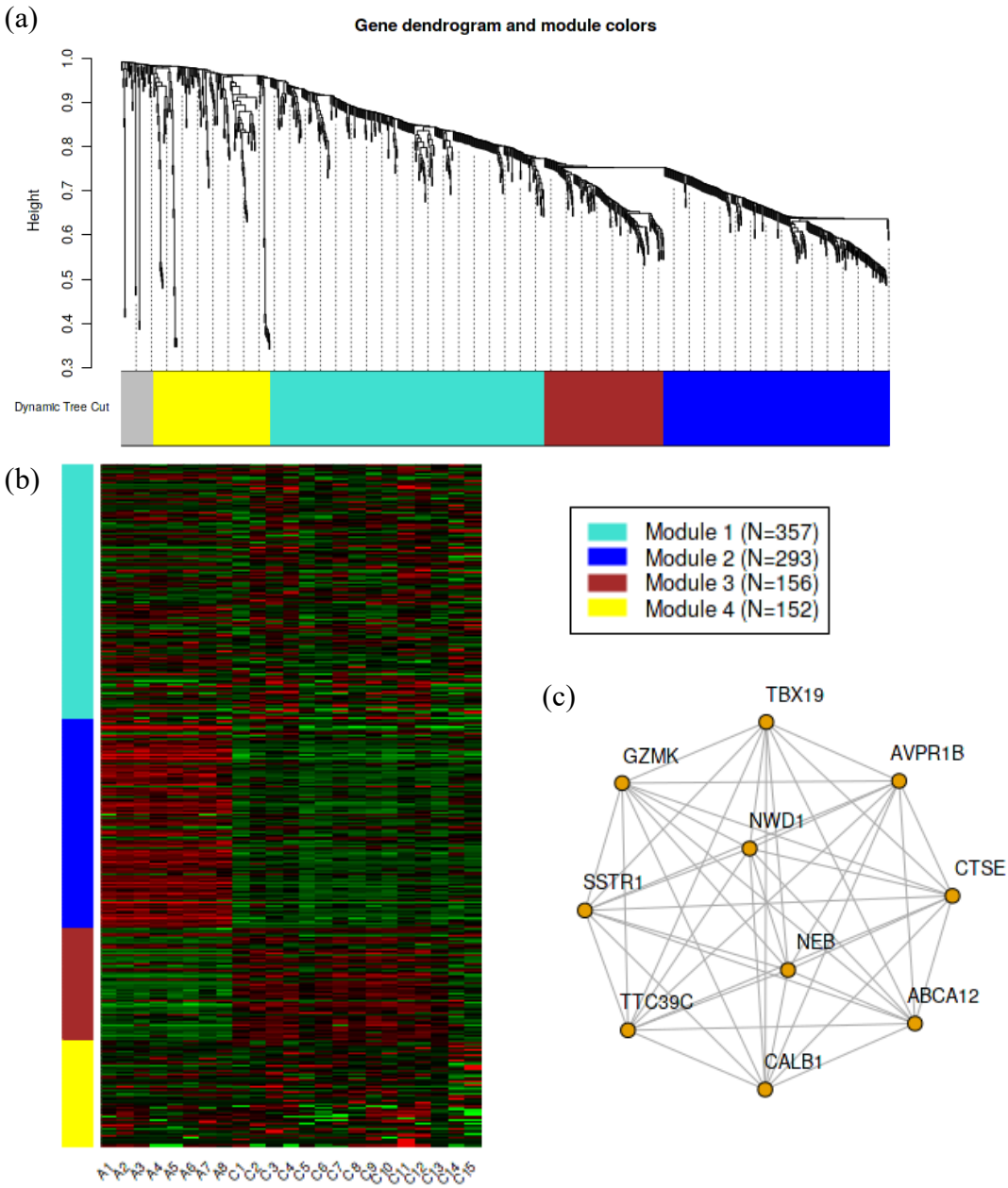

**Table 8.** Pathway enrichment analysis of gene list in blue module (n=293) in weighted gene coexpression network analysis (WGCNA)

| Pathways | Genes (n) | adjusted *P* |
|---|---|---|
| ***KEGG*** | | |
| Neuroactive ligand-receptor interaction | 16 | 6.10E-04 |
| Estrogen signaling pathway | 9 | 3.80E-03 |
| Cushing syndrome | 9 | 6.20E-03 |
| ***Reactome Pathway*** | | |
| R-HSA-112316 Neuronal System | 22 | 2.00E-07 |
| R-HSA-112315 Transmission across Chemical Synapses | 15 | 1.30E-05 |
| R-HSA-112314 Neurotransmitter receptors and postsynaptic signal transmission | 11 | 2.20E-04 |
| R-HSA-373752 Netrin-1 signaling | 6 | 2.00E-03 |
| R-HSA-1266738 Developmental Biology | 28 | 2.80E-03 |
| R-HSA-451307 Activation of Na-permeable kainate receptors | 2 | 5.10E-03 |
| R-HSA-422475 Axon guidance | 17 | 5.10E-03 |
| R-HSA-416476 G alpha (q) signalling events | 10 | 5.10E-03 |
| R-HSA-629597 Highly calcium permeable nicotinic acetylcholine receptors | 3 | 5.10E-03 |
| R-HSA-373760 L1CAM interactions | 7 | 5.10E-03 |
| R-HSA-397014 Muscle contraction | 10 | 5.10E-03 |
| R-HSA-418886 Netrin mediated repulsion signals | 3 | 5.10E-03 |
| R-HSA-1296071 Potassium Channels | 7 | 5.10E-03 |
| R-HSA-114508 Effects of PIP2 hydrolysis | 4 | 5.20E-03 |

From the results of the transcriptome analysis, I focused on the *AVPR1B* gene which encodes AVP receptor type 1B because *AVPR1B* was the most significantly different gene between SCAs and NCAs. I conducted the IHC staining for AVPR1B expression in 3 SCAs and 3 NCAs. **Figure 7** showed the representative images of IHC. The relative expression level of AVPR1B was higher in SCAs than NCAs.

**Figure 7.** The expression of AVPR1B in (a) SCAs and (b) NCAs using immunohistochemical staining. Representative images were shown. (original magnification: × 200);

(a)

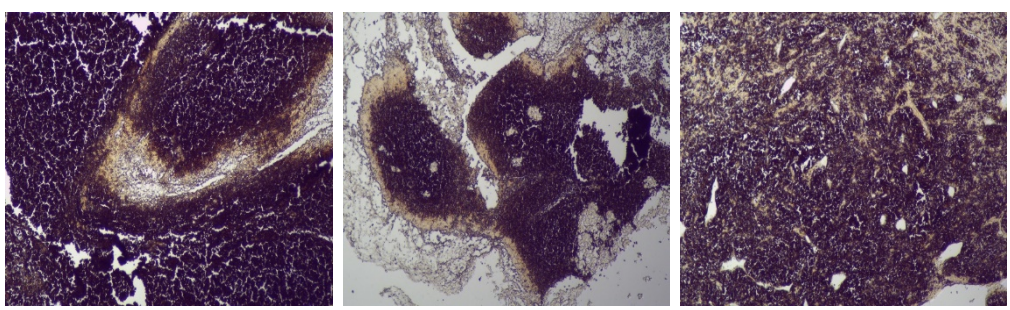

(b)

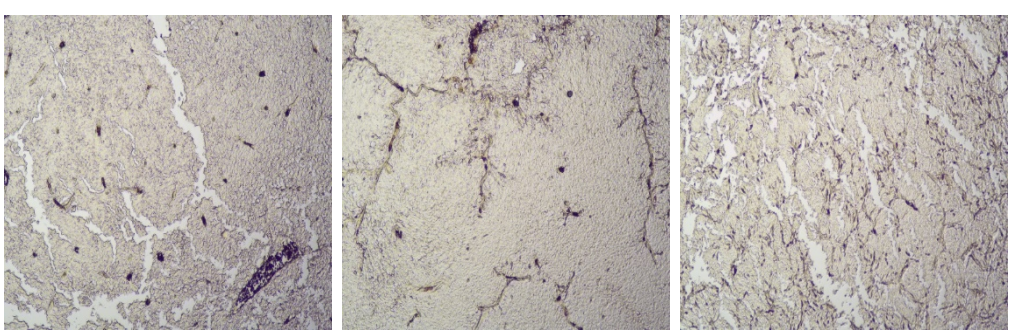

AVPR1B is known to be expressed in pituitary corticotroph adenomas cells and is related with autonomous ACTH secretion in Cushing's disease. I hypothesized that the AVRP1B may have a role in the aggressive behavior of SCAs as well as in ACTH secretion. To examine this hypothesis, I conducted a further study in *in vitro* cell lines. To examine the AVPR1B mRNA expression level in mouse corticotroph cell line AtT20 cells, relative quantification by qRT-PCR was compared with mouse myoblast C2C12 cells. AVPR1B gene was highly expressed in AtT 20 cells compared with C2C12 cells (**Figure 8(a)**). To examine the effect of AVPR1B expression on cell migration and invasion, I performed siRNA experiments in AtT20 cells. The efficiency of AVPR1B downregulation was up to 80% at 20 nM of siAVPR1B as shown by qRT-PCR (**Figure 8(b)**). At 20nM of siAVPR1B, POMC expression levels was also lowest at around 80% of siNC treatment groups (**Figure 8(c)**). Boyden chamber assay was implemented to examine the motility and invasiveness of siAVPR1B transfected cells (**Figure 9**). AVPR1B inhibition resulted in a significant decrease in AtT20 cell migration ($P$=0.049) and invasion ($P$=0.049). However, AVPR1B knockdown in AtT20 cells did not affect the cell proliferation ($P$=0.389).

**Figure 8.** AVPR1B knockdown decreases POMC expression in AtT20 cells. (a) AVPR1B was high expressed in AtT20 cells (b) siNC or siAVPR1B was transfected in AtT20 cell lines. AVPR1B is successfully knocked down with siRNA by 80% in AVPR1B mRNA expression at 20 nM. (c) AVPR1B knockdown decreases POMC mRNA expression by 80% at 20 nM. The data are summaries of three independent experiments performed in triplicates (*, $P<0.05$)

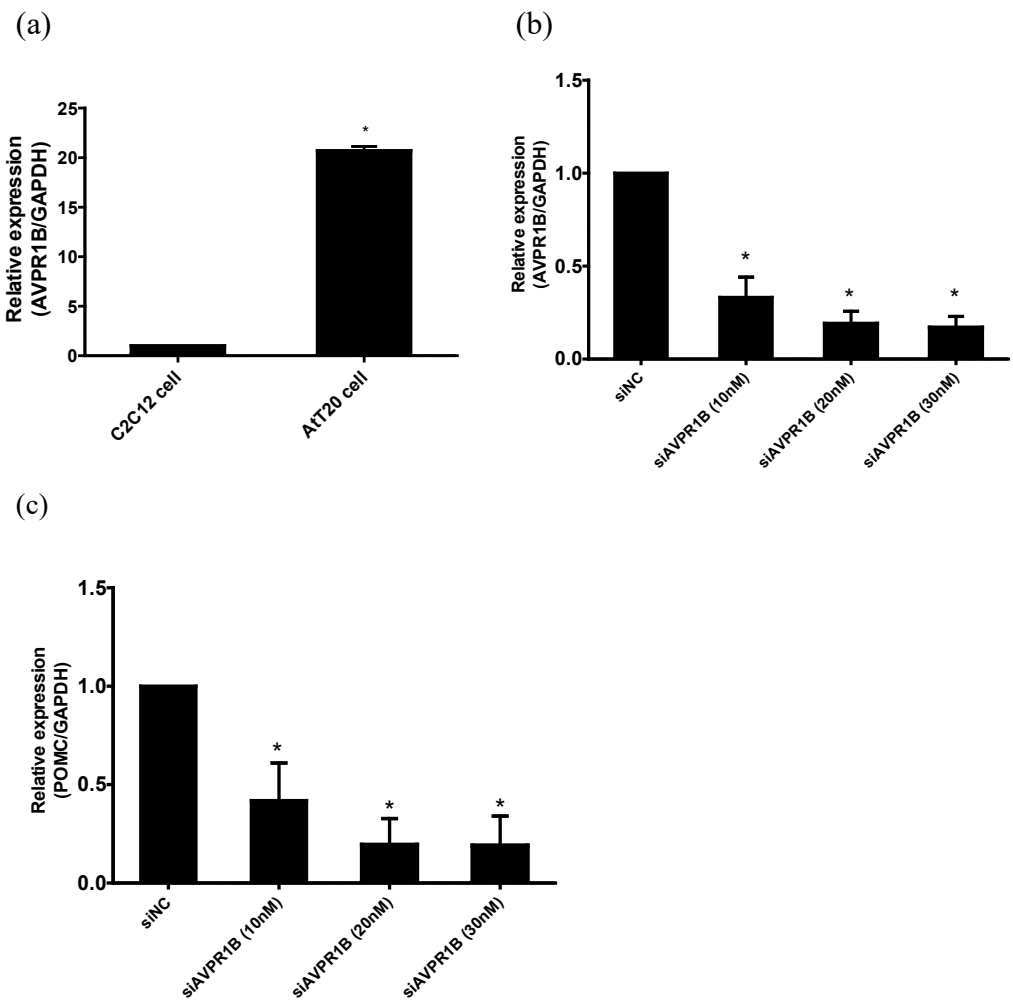

**Figure 9.** Depletion of AVPR1B does not affect proliferation but attenuate migration and invasion in AtT20 cells. (a) Knockdown of AVPR1B with siRNA in AtT20 cells does not affect proliferation. (b) Knockdown of AVPR1B with siRNA in AtT20 cells reduce the migration capacity. (c) Knockdown of AVPR1B with siRNA in AtT20 cells reduce invasion. The data are summaries of three independent experiments performed in triplicates (*, $P<0.05$)

(a)

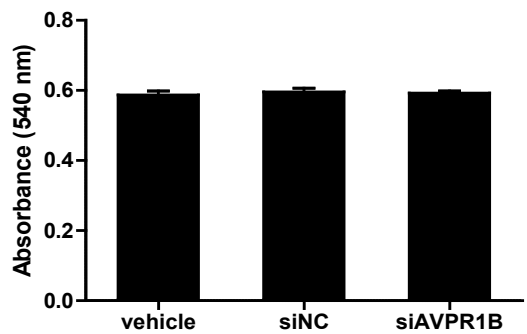


(b)

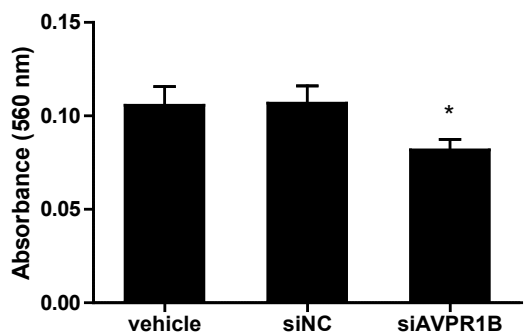


(c)

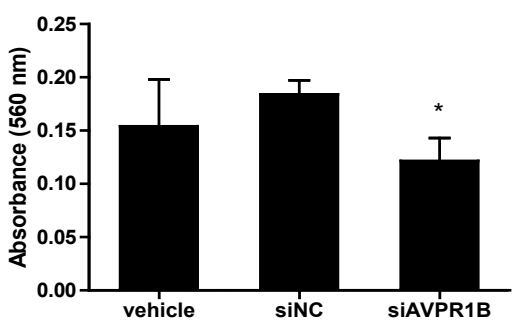

The effect of AVP and AVPR1B-specific antagonist, SSR149415 on the migration and invasion on AtT20 cells was examined (**Figure 10**). AtT20 cells serum-starved for 24 hours were treated with the indicated concentrations of vehicle, AVP and SSR149415. AVP and SSR149415 did not affect the cell proliferation (**Figure 10(a)**). In the migration assay, AVP enhanced the migration capacity of AtT20 cells whereas SSR149415 did not decrease the cell migration (**Figure 10(b)**). In the invasion assays, SSR149415 significantly inhibited the invasion capacity of AtT20 cells whereas AVP treatment did not show any difference in the invasion assay (**Figure 10(c)**). However, in the wound healing assays, the wound closure rate was not significantly different between AVP and SSR149415-treated group (**Figure 10(d)**).

**Figure 10.** AVPR1B antagonist, SSR149415 reduce the invasion capacity in AtT20 cells. (a) AVP and SSR149415 does not affect the cell proliferation capacity in MTT assays. (b) AVP increases the migration capacity in AtT20 cells. (c) AVP does not enhance the invasion capacity but SSR149415 inhibit the invasion in AtT20 cells. (d) The wound healing rate was not different between AVP and SSR149415-treated groups. Representative images were shown (*, $P$<0.05 compared with vehicle).

(a)

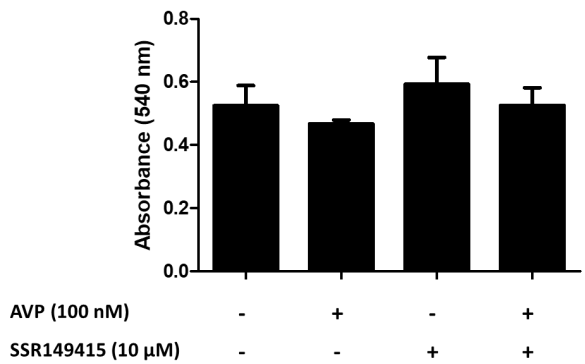


(b)

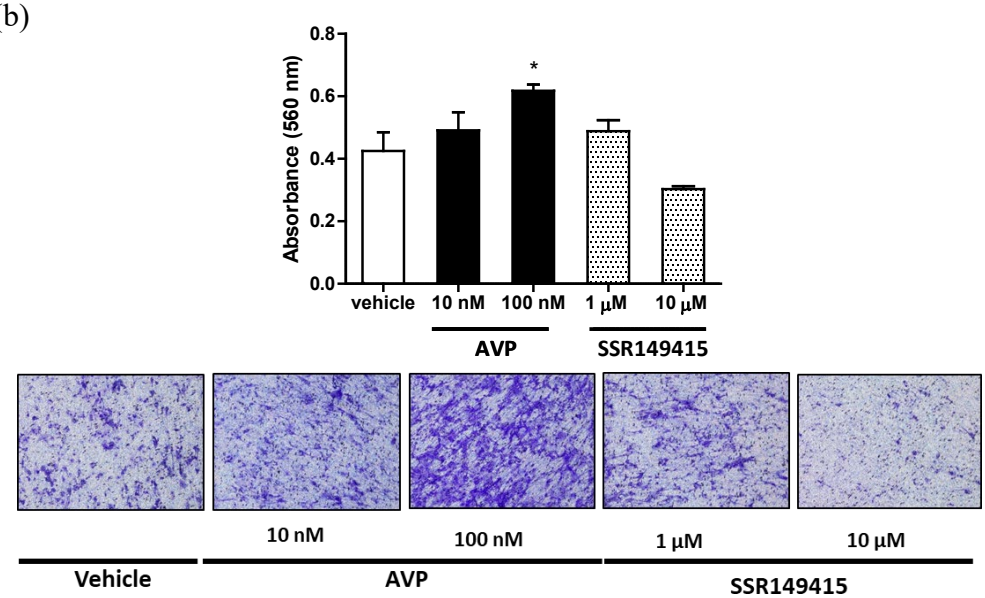

**(c)**

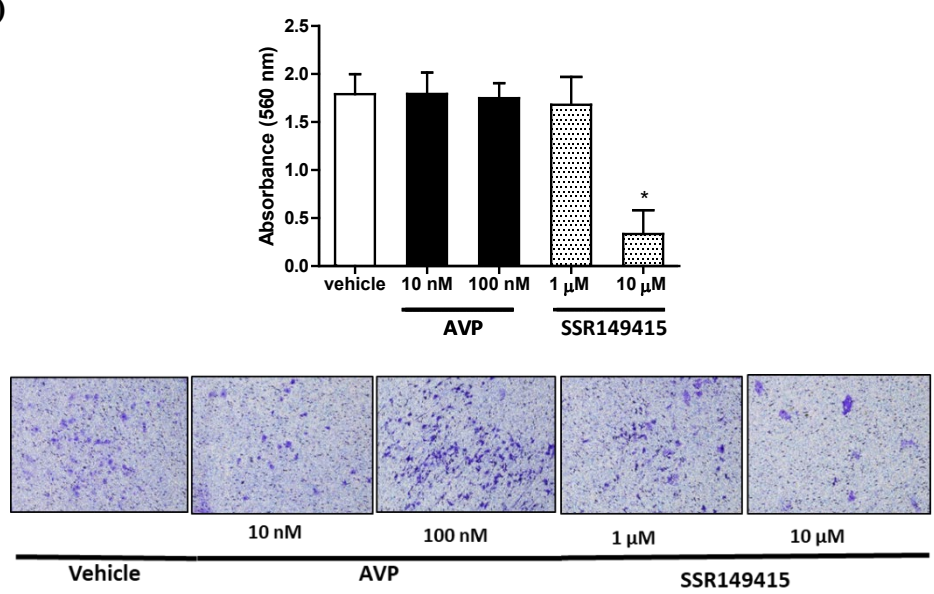
Absorbance (560 nm)
2.5
2.0
1.5
1.0
0.5
0.0
*
vehicle
10 nM
100 nM
1 µM
10 µM
AVP
SSR149415
10 nM
100 nM
1 µM
10 µM
Vehicle
AVP
SSR149415

**(d)**

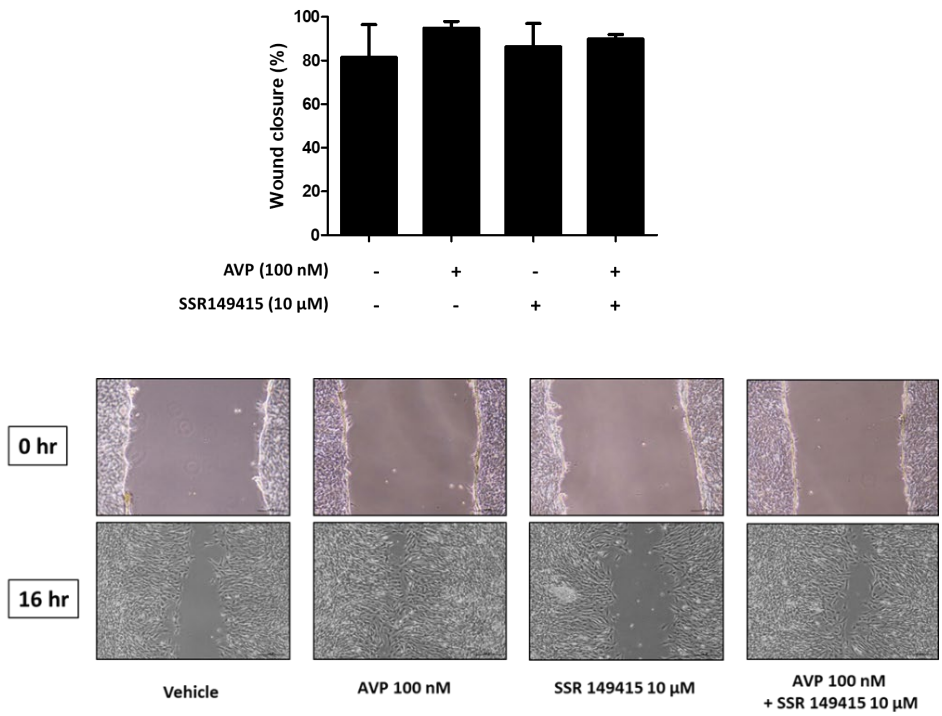
Wound closure (%)
100
80
60
40
20
0
AVP (100 nM) - + - +
SSR149415 (10 µM) - - + +
0 hr
16 hr
Vehicle
AVP 100 nM
SSR 149415 10 µM
AVP 100 nM
+ SSR 149415 10 µM

A part of MAPK pathways were activated in the transcriptome analysis. Then, I investigated whether AVPR1B signaling was mediated via ERK pathways (**Figure 11**). However, the ERK phosphorylation in AtT20 cells was not significantly different according to the concentration or duration of AVP treatment (**Figure 11 (a, b)**). ERK activation was inhibited at 10 μM of SSR149514, whereas ERK activation was not affected by AVP treatment **(Figure 11 (c))**.

**Figure 11.** ERK signaling mediates the AVPR1B signaling. (a) AtT20 cells were treated with 100 nM AVP for 0, 5, 10, and 20 min. (b) AtT20 cells were treated with AVP at 0, 1, 10, and 100 nM for 10 min. Epidermal growth factor (EGF) served as a positive control. (c) SSR129415 significantly inhibited ERK phosphorylation. The data are summaries of three independent experiments performed in triplicates. (*, $P < 0.05$ compared with vehicle-treated group; †, $P < 0.05$ compared with only AVP-treated group)

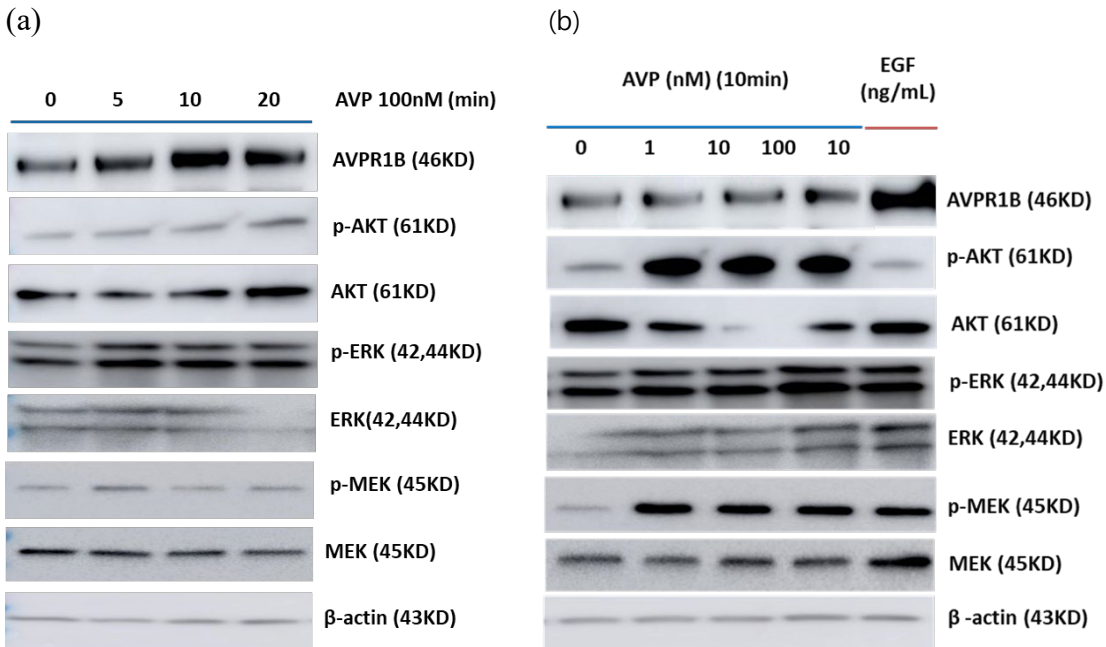

**(c)**

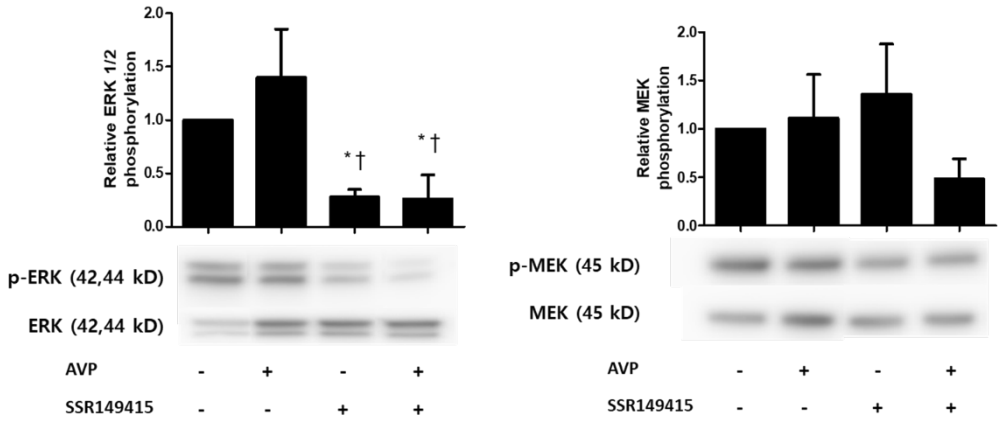
Relative ERK 1/2 phosphorylation
2.0
1.5
1.0
0.5
0.0
*†
*†
p-ERK (42,44 kD)
ERK (42,44 kD)
AVP - + - +
SSR149415 - - + +
Relative MEK phosphorylation
2.0
1.5
1.0
0.5
0.0
p-MEK (45 kD)
MEK (45 kD)
AVP - + - +
SSR149415 - - + +

**Supplemental Table 1.** Information of primers for qRT-PCR for validation of DEGs

| Primer name | Primer sequences | Primer size (bp) | Tm | Product size (bp) |
|---|---|---|---|---|
| hAR-F | ctgccagggaccatgttttg | 20 | 63.7 | 90 |
| hAR-R | agtgacacccagaagcttca | 20 | 58.4 | |
| hAVPR1B-F | cccctgatgaagattccacca | 21 | 64.4 | 96 |
| hAVPR1B-R | tgaagcccatgtagatccagg | 21 | 62.3 | |
| hDRD2-F | tcatgccctgggttgtctac | 20 | 60.9 | 103 |
| hDRD2-R | ctcgccgtgcacatcatg | 18 | 63.6 | |
| hEGFR-F | actcactctccataaatgctacg | 23 | 57.6 | 101 |
| hEGFR-R | ggagtcacccctaaatgcca | 20 | 62.2 | |
| hESR1-F | ggagatcttcgacatgctgc | 20 | 60.9 | 78 |
| hESR1-R | aggcacacaaactcctctcc | 20 | 59.3 | |
| hESR2-F | cccaaatgtgttgtggccaa | 20 | 64.9 | 113 |
| hESR2-R | gcgatcttgcttcacaccag | 20 | 62.0 | |
| hGATA2-F | ggctcgttcctgttcagaag | 20 | 60.0 | 137 |
| hGATA2-R | gtcggttctgcccattcatc | 20 | 62.8 | |
| hGHR-F | cgagttcagtgaggtgctct | 20 | 58.2 | 123 |
| hGHR-R | agcatcactgttagcccaaa | 20 | 58.4 | |
| hIGF1R-F | gtggggccaagagtgagat | 19 | 60.1 | 117 |
| hIGF1R-R | gagggttccacttcacgatt | 20 | 59.0 | |
| hPCSK2-F | gattgactatctccacccgg | 20 | 59.4 | 104 |
| hPCSK2-R | agtcatctgtgtaccgaggg | 20 | 57.6 | |
| hPOU1F1-F | aggaactcaggcggaaaagt | 20 | 60.2 | 142 |
| hPOU1F1-R | gcctccccaacatttgtctg | 20 | 62.8 | |
| hPTTG2-F | gaccaatggacccagaaaaca | 21 | 62.1 | 109 |
| hPTTG2-R | tggataggcgtcatctgagg | 20 | 61.2 | |
| hSSTR3-F | tctacatcctcaacctggcg | 20 | 61.2 | 148 |
| hSSTR3-R | ctggtgaactggttgatgcc | 20 | 61.5 | |
| hTBX19-F | ttcatagccgtgactgccta | 20 | 59.4 | 101 |
| hTBX19-R | tgatttctttccttggcatcca | 22 | 63.9 | |
| hTRHR-F | aaggaagcaggtcaccaaga | 20 | 59.8 | 111 |
| hTRHR-R | tggaaaggactggagagaaatga | 23 | 62.3 | |
| hVIPR1-F | gcctgtcccctcatcttcaa | 20 | 62.5 | 145 |
| hVIPR1-R | catccaaactcgctgccttg | 20 | 64.1 | |

**Supplemental Table 2.** Information of qRT-PCR primer sequences and target sequences of siRNAs

| Name | Primer sequences | Primer size (bp) | Tm | Product size (bp) |
|---|---|---|---|---|
| mAVPR1B (F) | gctggcccaagtcctcatcttctg | 24 | 63.4 | 103 |
| mAVPR1B (R) | gcggtgactcagggaacg t | 19 | 63.4 | |
| mPOMC (F) | gccagtgtcaggacctcac | 19 | 59.7 | 108 |
| mPOMC (R) | ggaacatgggagtctcggg | 19 | 59.7 | |
| siAVPR1B | gaguguauaggagagugua | 21 | | |
| | uacacucuccuauacacuc | 21 | | |

## DISCUSSION

In the present study, I investigated whether subjects with SCAs were at a higher risk of recurrence or progression compared to those with NCAs or other silent pituitary adenomas. I assumed that this biological behavior can be explained by transcriptome analysis. The GSEA demonstrated distinctive features of neuroactive ligand-receptor interactions, cancer-related signaling, and immune response-related pathway in SCAs. In advanced analysis including PAGE and WGCNA, I found that MAPK pathway and Gα(q) signaling pathway are activated in SCAs, which may be related with the aggressiveness of SCAs. The most distinguished gene among DEGs is AVPR1B. In *in vitro* study, AVPR1B knockdown did not affect the cell proliferation but mitigated the cell migration and invasiveness. Moreover, AVPR1B antagonist inhibit the cell invasiveness.

In 2017, the WHO classification of pituitary tumors indicated SCAs as “high-risk tumors” owing to their high probability of recurrence (7), although results from previous studies as to whether the clinical behavior of SCAs was more aggressive compared with other NFPAs were controversial. However, a recent systematic review including 10 eligible studies showed that there was no significant difference in recurrence rate ratios between SCAs and other NFPAs (29). In the present study, SCA subjects had about 3-fold higher risk of recurrence or progression than other NFPA subjects during a mean follow-up duration of 3.4 years. Therefore, I suggest that SCAs are associated with a

poor prognosis compared to other NFPAs. However, there was no significant difference between the two groups in terms of the Ki-67 proliferation index, tumor volume and cavernous sinus invasion at diagnosis. Previous studies also showed that Ki-67 was not related with SCAs recurrence rates or cavernous sinus invasion (11, 40). Hence, there may be other mechanisms explaining the biological behavior of SCAs.

To elucidate the mechanism of and aggressive behavior and hormone-silencing in SCAs, I performed an RNA sequencing analysis comparing gene expression profiling between SCAs and NCAs.

Several genes have been reported as potential markers for pituitary tumor invasiveness. The up-regulated fibroblast growth factor-4 (FGFR4) has been reported to correlate with the proliferation index Ki-67 and recurrence of overt Cushing's disease (41, 42). However, in the present study, *FGFR4* was rarely expressed in both SCAs and NCAs. Instead, *FGFR1* was one of the own-regulated genes in SCAs. *FGFR1* mutation has been reported to be involved in the normal migration of gonadotropin-releasing hormone fetal neurons and is a genetic cause of Kallmann syndrome (43, 44). FGFR1 may play a more critical role in NCAs instead of SCAs. As another growth factor receptor, the epidermal growth factor receptor (EGFR) was overexpressed in SCAs. Recently, EGFR was known to regulate ACTH secretion and corticotroph proliferation in ACTH-producing pituitary adenomas causing Cushing's disease (45, 46). Thus, EGFR may play a similar role in the

tumorigenesis of SCAs.

*PTTG* influences tumor invasiveness and recurrence in endocrine and non-endocrine tumors. In previous studies, PTTG was overexpressed in 90% of pituitary adenomas but was correlated with the Ki-67 index exhibited an aggressive behavior (47, 48). I found that *PTTG2* was overexpressed in SCAs but not in NCAs, but the absolute value of FPKM was only approximately 2.3.

Cell cycle regulators such as cyclin family have been implicated in tumorigenesis in cancers (49). Tani et al. suggested that reduced *CDKN2A* and upregulation of cyclin D1 gene expressions in SCAs prevents G1 phase cell cycle arrest and promote cell proliferation (30). However, in the present study, among cyclin dependent kinases/inhibitors, only *CDK18* was down-regulated ($\log_2|FC| = -2.36$, adjusted $P = 1.73E\text{-}7$) and *CDKN1A* was up-regulated in SCAs compared with NCAs ($\log_2|FC| = 2.49$, adjusted $P$=3.84E-5). Therefore, cell cycle regulators may not have a pivotal role in SCAs progression.

Several mechanisms have been suggested to explain the “silencing” of SCAs. I identified the different cell origins of SCAs. High expression levels of *TBX19 (TPIT),* and *POMC*, and low expression levels of *POU1F1 (PIT-1)*, *GATA2, NR5A1, NR0B1*, and *ESR1* confirmed the different cell origins of SCAs and NCAs (7). Regarding the genes related to POMC expressing, SCAs had a lower expression level of *PCSK2* but similar *PCSK1/*3 level to NCAs.

This finding is different to that reported in a study by Tateno et al. which showed lower expression level of *PCSK1/3* as well as *PCSK2* in SCAs than NFA by qRT-PCR (22). Both *PCSK1/3* and *PCSK2* are involved in the posttranslational processing of POMC. *PCSK1/3* cleaves POMC into mature ACTH (1-39) in anterior pituitary corticotroph cells, while *PCSK2* cleaves mature ACTH (1-39) into α-melanocytic stimulating hormone (α-MSH) and corticotropin-like intermediate lobe peptide (CLIP) in intermediate lobe of pituitary gland (50). Impaired POMC processing with reduced *PCSK1/3* results in accumulation of inactive POMC which make SCAs "silent". , less expression of *PCSK2* than NCAs make SCAs "ACTH-immunopositive."

The expression of somatostatin receptors (SSTRs) and dopamine receptor type 2 (D2R) were different between the two groups. Somatostatin expression was much higher in SCAs than in NCAs. *SSTR1* levels in SCAs were greater than NCAs whereas *SSTR3* levels in SCAs were lower than NCAs. However, *SSTR 2, 4,* and *5* were rarely expressed in both SCAs and NCAs. D2R was markedly greater in NCAs than SCAs. Somatostatin analogs selective for SSTR2-5 and dopamine agonist may have no therapeutic effect on SCAs.

*CRHR* and *AVPR1B* as specific receptors for ACTH secretagogues have been known to be overexpressed in corticotroph adenomas causing Cushing's disease. However, SCAs showed similar low expression levels of *CRHR1* and *2* but much higher expression levels of *AVPR1B* compared with NCAs in the present study. SCAs may produce ACTH responding to vasopressin but not

to CRH. In other words, low *CRHR* expression in SCAs may account for "silent" Cushing's syndrome. Tateno et al. also reported that *AVPR1B* mRNA expression levels in overt corticotroph adenomas and SCAs were about 15- and 5-fold higher than those in NCAs, respectively (22).

In further network and pathway analysis, I found that the MAPK cascade was activated in SCAs and AVPR1B was the most distinctive gene between SCAs and NCAs. Moreover, another study has shown that the activation of *AVPR1B* may lead to activation of the cAMP signaling pathway and MAPK cascade to induce tumor growth (51). In this context, I focused on the effect of AVPR1B on SCA progression and growth. Among three vasopressin receptor subtypes including AVPR1A, AVPR1B, and AVPR2, AVPR1B is expressed exclusively in pituitary corticotroph cells (52). AVPR1B is the subfamily of G-protein coupled receptors, which produces signals via G proteins $G_{q/11}$ to stimulate a phospholipase C (PLC) thereby triggering phosphoinositide hydrolysis, calcium mobilization and protein kinase C (53). Thibonner et al. suggested that AVPR1B was linked to more than one G protein signal transduction pathway. In low density of AVPR1B, only $G_{q/11}$ involved PLC and Ras/RAF/MEK/ERK pathway activation to induce tumor growth (51). I demonstrated the ERK pathway was activated in AVP-treated group, MEK phosphorylation was not significantly different in AVP or SSR129415-treated group. However, high levels of AVPR1B expression may couple to both stimulatory and inhibitory signals recruiting Gs, Gi, and Gq/11 classes,

leading to high cAMP production (51). As the same member of vasopressin/oxytocin family, the similar GPCR signaling pathway of AVPR1A has been reported to be implicated in poor prostate cancer prognosis (54).

To demonstrate the role of AVPR1B in SCAs, I conducted an *in vitro* assay in a mouse corticotroph cell lines AtT20. However, Ventura et al. used reverse transcription polymerase chain reaction (RT-PCR) to demonstrate the expression of AVPR1B was very low in AtT20 cells (55). In the present study, using qRT-PCR, I evaluated the expression of AVPR1B genes quantitatively in AtT20 cells although the cycle threshold (Ct) values of AVPR1B in AtT20 cells were around 32−35 (data not shown). In addition, I showed that AtT20 cells expressed sufficient AVPR1B protein and were enhanced by AVP treatment using Western blot. This finding is consistent with that from a previous study, which showed that AVP contributes to the AVPR1B upregulation by increasing the GAGA binding activity to the AVPR1B promoter (56).

After I knocked down *AVPR1B* in AtT20 cells, I figured out that proliferation was not affected but migratory capacity and invasiveness was affected in SCAs. AVP increase the migration capacity and antagonizing AVPR1B significantly suppressed the invasive capacity of AtT20 cells. Therefore, AVPR1B might have a role in the progression and growth of SCAs. However, in the wound healing assays, SSR149415 tended to inhibit the wound closure

rate, but the result was not significant. This discrepancy may be attributed to the characteristics of the wound healing assay. The wound healing assay reflects the cell proliferation as well as migration capacity. As above-mentioned, I showed the little effect of AVPR1B on cell proliferation. Thus, the similar capacity of cell proliferation might overcome the cell migration capacity in the wound healing assay.

This study had several limitations. To elucidate the mechanism of biological behaviors, *i.e.*, silencing, the gene expression profiling of SCAs should be compared with ACTH-producing pituitary adenomas causing Cushing's disease as well as NCAs. However, we could not obtain fresh frozen tissues of ACTH-producing pituitary adenomas causing Cushing's disease due to very small adenoma size. All significant DEGs were not evaluated in qRT-PCR or functional studies. Moreover, the mechanisms explaining how AVPR1B knockdown affects the migration and invasion capacity of AtT20 cells should need further examination.

## CONCLUSION

Subjects with SCAs were at a high risk of recurrence or progression after primary surgery compared to those with non-SCAs. AVPR1B may play a significant role in the aggressive behavior as well as ACTH-immunopositivity in SCAs. AVPR1B may be a novel therapeutic target in subjects with SCAs.

## REFERENCES

1. Daly AF, Rixhon M, Adam C, Dempegioti A, Tichomirowa MA, Beckers A. High prevalence of pituitary adenomas: a cross-sectional study in the province of Liege, Belgium. J Clin Endocrinol Metab. 2006;91(12):4769-75.

2. Kim YH, Song SW, Lee JY, Kim JW, Kim YH, Phi JH, et al. Surgically treated brain tumors: a retrospective case series of 10,009 cases at a single institution. World Neurosurg. 2011;76(6):555-63.

3. Fernandez A, Karavitaki N, Wass JA. Prevalence of pituitary adenomas: a community-based, cross-sectional study in Banbury (Oxfordshire, UK). Clin Endocrinol (Oxf). 2010;72(3):377-82.

4. Raappana A, Koivukangas J, Ebeling T, Pirila T. Incidence of pituitary adenomas in Northern Finland in 1992-2007. J Clin Endocrinol Metab. 2010;95(9):4268-75.

5. Raverot G, Burman P, McCormack A, Heaney A, Petersenn S, Popovic V, et al. European Society of Endocrinology Clinical Practice Guidelines for the management of aggressive pituitary tumours and carcinomas. Eur J Endocrinol. 2018;178(1):G1-G24.

6. Raverot G, Jouanneau E, Trouillas J. Management of endocrine disease: clinicopathological classification and molecular markers of pituitary tumours for personalized therapeutic strategies. Eur J Endocrinol. 2014;170(4):R121-32.

7. Inoshita N, Nishioka H. The 2017 WHO classification of pituitary adenoma:

overview and comments. Brain Tumor Pathol. 2018;35(2):51-6.

8. Molitch ME. Diagnosis and Treatment of Pituitary Adenomas: A Review. JAMA. 2017;317(5):516-24.

9. Korbonits M, Carlsen E. Recent clinical and pathophysiological advances in non-functioning pituitary adenomas. Horm Res. 2009;71 Suppl 2:123-30.

10. Kovacs K, Horvath E, Bayley TA, Hassaram ST, Ezrin C. Silent corticotroph cell adenoma with lysosomal accumulation and crinophagy. A distinct clinicopathologic entity. Am J Med. 1978;64(3):492-9.

11. Yamada S, Ohyama K, Taguchi M, Takeshita A, Morita K, Takano K, et al. A study of the correlation between morphological findings and biological activities in clinically nonfunctioning pituitary adenomas. Neurosurgery. 2007;61(3):580-4; discussion 4-5.

12. Cho HY, Cho SW, Kim SW, Shin CS, Park KS, Kim SY. Silent corticotroph adenomas have unique recurrence characteristics compared with other nonfunctioning pituitary adenomas. Clin Endocrinol (Oxf). 2010;72(5):648-53.

13. Langlois F, Lim DST, Varlamov E, Yedinak CG, Cetas JS, McCartney S, et al. Clinical profile of silent growth hormone pituitary adenomas; higher recurrence rate compared to silent gonadotroph pituitary tumors, a large single center experience. Endocrine. 2017;58(3):528-34.

14. Ben-Shlomo A, Cooper O. Silent corticotroph adenomas. Pituitary. 2018;21(2):183-93.

15. Cheres AF, ElAsmar N, Rajpal A, Selman WR, Arafah BM. Perioperative hypothalamic pituitary adrenal function in patients with silent corticotroph adenomas. Pituitary. 2017;20(4):471-6.

16. Horvath E, Kovacs K, Lloyd RV. Pars intermedia of the human pituitary revisited: Morphologic aspects and frequency of hyperplasia of POMC-peptide immunoreactive cells. Endocrine Pathology. 1999;10(1):55-64.

17. Matsuno A, Okazaki R, Oki Y, Nagashima T. Secretion of high-molecular-weight adrenocorticotropic hormone from a pituitary adenoma in a patient without Cushing stigmata. Case report. J Neurosurg. 2004;101(5):874-7.

18. Raverot G, Wierinckx A, Jouanneau E, Auger C, Borson-Chazot F, Lachuer J, et al. Clinical, hormonal and molecular characterization of pituitary ACTH adenomas without (silent corticotroph adenomas) and with Cushing's disease. Eur J Endocrinol. 2010;163(1):35-43.

19. Tateno T, Izumiyama H, Doi M, Akashi T, Ohno K, Hirata Y. Defective expression of prohormone convertase 1/3 in silent corticotroph adenoma. Endocr J. 2007;54(5):777-82.

20. Jahangiri A, Wagner JR, Pekmezci M, Hiniker A, Chang EF, Kunwar S, et al. A comprehensive long-term retrospective analysis of silent corticotrophic adenomas vs hormone-negative adenomas. Neurosurgery. 2013;73(1):8-17; discussion -8.

21. Artenstein AW, Opal SM. Proprotein convertases in health and disease. N Engl J Med. 2011;365(26):2507-18.

22. Tateno T, Izumiyama H, Doi M, Yoshimoto T, Shichiri M, Inoshita N, et al. Differential gene expression in ACTH -secreting and non-functioning pituitary tumors. Eur J Endocrinol. 2007;157(6):717-24.

23. Drummond J, Roncaroli F, Grossman AB, Korbonits M. Clinical and Pathological Aspects of Silent Pituitary Adenomas. J Clin Endocrinol Metab. 2019;104(7):2473-89.

24. Nishioka H, Inoshita N, Mete O, Asa SL, Hayashi K, Takeshita A, et al. The Complementary Role of Transcription Factors in the Accurate Diagnosis of Clinically Nonfunctioning Pituitary Adenomas. Endocr Pathol. 2015;26(4):349-55.

25. Oystese KA, Casar-Borota O, Normann KR, Zucknick M, Berg JP, Bollerslev J. Estrogen Receptor alpha, a Sex-Dependent Predictor of Aggressiveness in Nonfunctioning Pituitary Adenomas: SSTR and Sex Hormone Receptor Distribution in NFPA. J Clin Endocrinol Metab. 2017;102(9):3581-90.

26. Cooper O, Ben-Shlomo A, Bonert V, Bannykh S, Mirocha J, Melmed S. Silent corticogonadotroph adenomas: clinical and cellular characteristics and long-term outcomes. Horm Cancer. 2010;1(2):80-92.

27. Ratnasingam J, Lenders N, Ong B, Boros S, Russell AW, Inder WJ, et al. Predictors for secondary therapy after surgical resection of nonfunctioning pituitary adenomas. Clin Endocrinol (Oxf). 2017;87(6):717-24.

28. Tampourlou M, Ntali G, Ahmed S, Arlt W, Ayuk J, Byrne JV, et al.

Outcome of Nonfunctioning Pituitary Adenomas That Regrow After Primary Treatment: A Study From Two Large UK Centers. J Clin Endocrinol Metab. 2017;102(6):1889-97.

29. Fountas A, Lavrentaki A, Subramanian A, Toulis KA, Nirantharakumar K, Karavitaki N. Recurrence in silent corticotroph adenomas after primary treatment: A systematic review and meta-analysis. J Clin Endocrinol Metab. 2019;104(4):1039–48.

30. Tani Y, Inoshita N, Sugiyama T, Kato M, Yamada S, Shichiri M, et al. Upregulation of CDKN2A and suppression of cyclin D1 gene expressions in ACTH-secreting pituitary adenomas. Eur J Endocrinol. 2010;163(4):523-9.

31. Righi A, Jin L, Zhang S, Stilling G, Scheithauer BW, Kovacs K, et al. Identification and consequences of galectin-3 expression in pituitary tumors. Mol Cell Endocrinol. 2010;326(1-2):8-14.

32. Riss D, Jin L, Qian X, Bayliss J, Scheithauer BW, Young WF, Jr., et al. Differential expression of galectin-3 in pituitary tumors. Cancer Res. 2003;63(9):2251-5.

33. Knosp E, Steiner E, Kitz K, Matula C. Pituitary adenomas with invasion of the cavernous sinus space: a magnetic resonance imaging classification compared with surgical findings. Neurosurgery. 1993;33(4):610-7; discussion 7-8.

34. Dobin A, Davis CA, Schlesinger F, Drenkow J, Zaleski C, Jha S, et al. STAR: ultrafast universal RNA-seq aligner. Bioinformatics. 2013;29(1):15-

21.

35. Li B, Dewey CN. RSEM: accurate transcript quantification from RNA-Seq data with or without a reference genome. BMC Bioinformatics. 2011;12:323.

36. Ge SX, Son EW, Yao R. iDEP: an integrated web application for differential expression and pathway analysis of RNA-Seq data. BMC Bioinformatics. 2018;19(1):534.

37. Subramanian A, Tamayo P, Mootha VK, Mukherjee S, Ebert BL, Gillette MA, et al. Gene set enrichment analysis: a knowledge-based approach for interpreting genome-wide expression profiles. Proc Natl Acad Sci U S A. 2005;102(43):15545-50.

38. Slenter DN, Kutmon M, Hanspers K, Riutta A, Windsor J, Nunes N, et al. WikiPathways: a multifaceted pathway database bridging metabolomics to other omics research. Nucleic Acids Res. 2018;46(D1):D661-D7.

39. Fabregat A, Jupe S, Matthews L, Sidiropoulos K, Gillespie M, Garapati P, et al. The Reactome Pathway Knowledgebase. Nucleic Acids Res. 2018;46(D1):D649-D55.

40. Langlois F, Lim DST, Yedinak CG, Cetas I, McCartney S, Cetas J, et al. Predictors of silent corticotroph adenoma recurrence; a large retrospective single center study and systematic literature review. Pituitary. 2018;21(1):32-40.

41. Qian ZR, Sano T, Asa SL, Yamada S, Horiguchi H, Tashiro T, et al.

Cytoplasmic expression of fibroblast growth factor receptor-4 in human pituitary adenomas: relation to tumor type, size, proliferation, and invasiveness. J Clin Endocrinol Metab. 2004;89(4):1904-11.

42. Brito LP, Lerario AM, Bronstein MD, Soares IC, Mendonca BB, Fragoso MC. Influence of the fibroblast growth factor receptor 4 expression and the G388R functional polymorphism on Cushing's disease outcome. J Clin Endocrinol Metab. 2010;95(10):E271-9.

43. Villanueva C, de Roux N. FGFR1 mutations in Kallmann syndrome. Front Horm Res. 2010;39:51-61.

44. Correa FA, Trarbach EB, Tusset C, Latronico AC, Montenegro LR, Carvalho LR, et al. FGFR1 and PROKR2 rare variants found in patients with combined pituitary hormone deficiencies. Endocr Connect. 2015;4(2):100-7.

45. Fukuoka H, Cooper O, Ben-Shlomo A, Mamelak A, Ren SG, Bruyette D, et al. EGFR as a therapeutic target for human, canine, and mouse ACTH-secreting pituitary adenomas. J Clin Invest. 2011;121(12):4712-21.

46. Araki T, Liu X, Kameda H, Tone Y, Fukuoka H, Tone M, et al. EGFR Induces E2F1-Mediated Corticotroph Tumorigenesis. J Endocr Soc. 2017;1(2):127-43.

47. Salehi F, Kovacs K, Scheithauer BW, Lloyd RV, Cusimano M. Pituitary tumor-transforming gene in endocrine and other neoplasms: a review and update. Endocr Relat Cancer. 2008;15(3):721-43.

48. Filippella M, Galland F, Kujas M, Young J, Faggiano A, Lombardi G, et

al. Pituitary tumour transforming gene (PTTG) expression correlates with the proliferative activity and recurrence status of pituitary adenomas: a clinical and immunohistochemical study. Clin Endocrinol (Oxf). 2006;65(4):536-43.

49. Malumbres M, Barbacid M. To cycle or not to cycle: a critical decision in cancer. Nat Rev Cancer. 2001;1(3):222-31.

50. Takumi I, Steiner DF, Sanno N, Teramoto A, Osamura RY. Localization of prohormone convertases 1/3 and 2 in the human pituitary gland and pituitary adenomas: analysis by immunohistochemistry, immunoelectron microscopy, and laser scanning microscopy. Mod Pathol. 1998;11(3):232-8.

51. Thibonnier M, Preston JA, Dulin N, Wilkins PL, Berti-Mattera LN, Mattera R. The human V3 pituitary vasopressin receptor: ligand binding profile and density-dependent signaling pathways. Endocrinology. 1997;138(10):4109-22.

52. Birnbaumer M. Vasopressin receptors. Trends Endocrinol Metab. 2000;11(10):406-10.

53. Koshimizu TA, Nakamura K, Egashira N, Hiroyama M, Nonoguchi H, Tanoue A. Vasopressin V1a and V1b receptors: from molecules to physiological systems. Physiol Rev. 2012;92(4):1813-64.

54. Zhao N, Peacock SO, Lo CH, Heidman LM, Rice MA, Fahrenholtz CD, et al. Arginine vasopressin receptor 1a is a therapeutic target for castration-resistant prostate cancer. Sci Transl Med. 2019;11(498).

55. Ventura MA, Rene P, de Keyzer Y, Bertagna X, Clauser E. Gene and

cDNA cloning and characterization of the mouse V3/V1b pituitary vasopressin receptor. J Mol Endocrinol. 1999;22(3):251-60.

56. Volpi S, Liu Y, Aguilera G. Vasopressin increases GAGA binding activity to the V1b receptor promoter through transactivation of the MAP kinase pathway. J Mol Endocrinol. 2006;36(3):581-90.

# 국 문 초 록

배경: 무증상 ACTH 분비선종은 임상적으로는 비기능성 뇌하수체선종으로 발현하고 고코르티솔혈증의 생화학적, 임상적 증상 없이 ACTH 면역조직화학염색에 양성 소견을 보인다. 무증상 ACTH 분비선종은 대개 종괴 효과에 의한 증상과 공격적인 질환 경과를 나타낸다. 본 연구에서는 무증상 ACTH 분비선종의 예후를 알아보고 영세포선종과 유전자 발현 양상을 비교하며 전사체 분석에서 밝혀진 AVPR1B 의 역할을 규명하고자 한다.

방법: 임상 연구에는 일차 경접형동 수술을 받고 임상적으로 비기능성 뇌하수체선종으로 발현한 433명의 연구대상자를 포함하였다. 이들의 임상적, 생화학적, 영상학적, 면역조직화학염색 결과를 의무기록을 통해 확인하고 무증상 ACTH 분비선종인 환자와 아닌 환자를 비교하였다. 수술 후 재발 혹은 진행 위험은 Cox 비례 위험 회귀 모형을 통해 분석하였다. 전사체 분석으로는 신선동결조직이 보관되어 있는 8례의 무증상 ACTH 분비선종과 15례의 영세포선종에서 Illumina 플랫폼을 이용한 RNA 염기서열분석을 시행하였다. 두 군에서 나타나는 차별발현유전자에 대해서는 유전자 온톨로지, 신호전달 경로, 네트워크 분석을 시행하였다. 마우스 뇌하수체 ACTH 분비세포인 AtT20 세포에서 AVPR1B siRNA 형질주입 후 증식, 이동, 침습 정도를 확인하였다. 또한 AVP와 AVPR1B 길항제인 SSR149415 처리한 후 AtT20 세포에서

증식, 이동, 침습 정도를 살펴보았다.

결과: 임상적으로 비기능성 뇌하수체선종 433명 중 무증상 ACTH 분비선종은 총 69명이었다. 이들 중에는 여성이 많았고 아침 혈장 ACTH 와 코르티솔 수치가 다소 높았다. 하지만 종양 부피와 해면동침범, Ki-67 지수 등에서는 두 군간 차이가 없었다. 무증상 ACTH 분비선종군은 무증상 ACTH 분비선종이 아닌 군에 비해 재발 혹은 진행 위험이 3.3 배 높았다. RNA 염기서열분석을 통해 약 1,695개의 차별발현유전자를 확인하였다. 무증상 ACTH 분비선종에서는 *TBX19, AVPR1B, EGFR, POMC* 발현이 높았고 *POU1F1 (Pit-1), GATA2, NR5A1 (SF-1), NR0B1 (DAX1), DRD2, SSTR3, PCSK2* 발현이 낮았다. 추가 분석에서 무증상 ACTH 분비선종에서는 면역반응이나 종양 관련 신호전달경로 및 MAPK, $G_{\alpha}(q)$ 신호전달경로가 활성화되었으며 펩티드호르몬 처리 과정과 세포외기질형성 관련 경로는 억제되어 있었다. AtT20 세포에서 AVPR1B 발현을 억제시킨 결과 세포 증식에는 영향이 없었고 ACTH 분비, 이동, 침습 능력이 떨어졌음을 확인하였다. 또한 AtT20 세포에서 AVP 처리 후에는 이동 능력이 증가하고 SSR149415 처리 후에는 침습 능력이 떨어짐을 확인하였다.

결론: 무증상 ACTH 분비선종 환자는 다른 비기능선 뇌하수체선종에 비해 재발 및 진행 위험이 높다. 무증상 ACTH 분비선종에서 AVPR1B 은 ACTH 면역조직화학염색 양성 소견뿐만 아니라 공격적인 임상양상과

관련 있을 수 있다. AVPR1B 는 치료에 반응하지 않는 무증상 ACTH 분비선종의 새로운 치료 타겟이 될 수 있다.

주요어: 무증상 ACTH 분비 선종, 임상적으로는 비기능성 뇌하수체 선종, 영세포선종, ACTH, AVPR1B

학번: 2012-30797